Simultaneous measurements of new particle formation in one-second time resolution at a street site and a rooftop site

Yujiao Zhu[1#], Caiqing Yan[2#], Renyi Zhang[2,3], Zifa Wang[4], Mei Zheng[2], Huiwang Gao[1], Yang Gao[1], Xiaohong Yao[1,5*]

[1]Key Lab of Marine Environmental Science and Ecology, Ministry of Education, Ocean University of China, Qingdao 266100, China

[2]State Key Joint Laboratory for Environmental Simulation and Pollution Control, College of Environmental Sciences and Engineering, Peking University, Beijing 100871, China

[3]Departments of Atmospheric Sciences and Chemistry, Center for the Atmospheric Chemistry and the Environment, Texas A&M University, College Station, TX 77843, USA

[4] State Key Laboratory of Atmospheric Boundary Layer Physics and Atmospheric Chemistry (LAPC), Institute of Atmospheric Physics, Chinese Academy of Sciences, Beijing, China

[5]Qiangdao Collaborative Center of Marine Science and Technology, Qingdao 266100, China

[#] both have the same contribution, * *Correspondence to*: Xiaohong Yao, Phone: (86) 532-66782565; Fax: 86-532-66782810; Email address: xhyao@ouc.edu.cn

Abstract

This study is the first to use two identical Fast Mobility Particle Sizers for simultaneous measurement of particle number size distributions (PNSDs) at a street site and a rooftop site within 500 m distance in winter and spring times to investigate new particle formation (NPF) in Beijing. The collected datasets in one-second time resolution allow deduction of the freshly emitted traffic particle signal from the measurements at the street site and thereby enable the evaluation of the effects on NPF in an urban atmosphere through a site-by-site comparison. The number concentrations of 8 nm to 20 nm newly formed particles and the apparent formation rate (FR) in the springtime were smaller at the street site than at the rooftop site. In contrast, NPF was enhanced in the wintertime at the street site with FR increased by a factor of 3 to 5 times, characterized by a shorter NPF time and higher new particle yields than at the rooftop site. Our results imply that the street canyon likely exerts distinct effects on NPF under warm or cold ambient temperature conditions because of on-road vehicle emissions, i.e., stronger condensation sinks that may be responsible for the reduced NPF in the springtime but efficient nucleation and partitioning of gaseous species that contribute to the enhanced NPF in the wintertime. The occurrence or absence of apparent growth for new particles with mobility diameters larger than 10 nm was also analyzed. The oxidization of biogenic organics in the presence of strong photochemical reactions is suggested to play an important role in growing new particles with diameters larger than 10 nm, but sulfuric acid is unlikely to be the main species for the apparent growth. However, the number of datasets used in this study is relatively small, and larger datasets are essential to draw a general conclusion.

Keywords: new particle formation, street site, enhanced nucleation, vehicle emissions, semivolatile organics

1. Introduction

New particle formation (NPF) has been measured under diverse environmental conditions, accounting for approximately 50% of the aerosol number production in the troposphere, but the chemical mechanism and species leading to aerosol nucleation and growth remain highly uncertain (Merikanto et al., 2009; Yao et al., 2010; Zhang et al., 2012). NPF occurs in two distinct stages, i.e., nucleation to form the critical nuclei and the subsequent growth of freshly nucleated particles to larger sizes (Kulmala et al., 2004, 2013; Zhang, 2010; Zhang et al., 2012). In addition, the growth process competes with capture/removal of nanoparticles by coagulation with pre-existing aerosols. Currently, considerable uncertainty exists concerning the mechanism and the identity of chemical species responsible for aerosol nucleation and growth (Zhang et al., 2012; Wang et al., 2017). Sulfuric acid has been commonly considered one of the main precursors of aerosol nucleation and growth, but the presence of sulfuric acid is insufficient to explain the observed NPF under various ambient conditions (Kulmala et al., 2004; Kulmala and Kerminen, 2008; Zhang et al., 2012). Earlier studies indicated that NH_3 can enhance aerosol nucleation, but recent laboratory experimental and theoretical studies have suggested that amines and highly oxygenated molecules (HOMs) play vital roles in enhancing nucleation and promoting the initial growth of newly formed particles in the atmosphere (Zhang et al., 2004, 2009, 2012; Wang et al., 2010; Riipinen et al., 2011; Kulmala et al., 2013; Qiu and Zhang, 2013; Schobesberger et al., 2013; Ehn et al., 2014; Riccobono et al., 2014; Tröstl et al., 2016). Therefore, it is critical to evaluate the effects of nucleating species other than sulfuric acid and the dependence of NPF on pre-existing particles in the atmosphere. Urban street canyons provide semi-enclosed environments, trapping vehicle exhaust that likely contains aromatic and aliphatic hydrocarbons, SO_2, NOx, amines, black carbon, etc. (Pierson et al., 1983; Stemmler et al., 2005; Burgard et al., 2006; Liu et al., 2008; Buccolieri et al., 2009; Gentner, et al., 2012; Sun et al., 2012), thus serving effectively as environmental chambers to investigate the effects of on-road vehicle emissions, i.e., gaseous species and primary particles, on NPF.

A major challenge exists for studying NPF at street sites because of the interference from primarily emitted vehicular particles. The primary particles can be generated directly in the engine during fuel combustion or can be nucleated in the air during dilution and cooling of hot exhaust (Kittelson, 1998; Kittelson et al., 2008; Arnold et al., 2012; Rönkkö et al., 2013; Vu et al., 2015). The former primary particles consist mostly of soot and exist mainly in the Aitken mode and accumulation

mode, ranging from 30 nm to 500 nm, and the freshly nucleated vehicular particles during the initial 1-2 s of exhaust cooling and dilution processes reportedly exhibit a nucleation mode at 10-20 nm (Shi et al., 2000; Zhu et al., 2002a,b, 2006; Vu et al., 2015). The particle number concentration (PNC) at the roadside can vary significantly, depending on the traffic flow, composition and speed as well as wind speed and direction (Yao et al., 2005). The Scanning Mobility Particle Sizer (SMPS) and other scanning sizers, e.g., commonly operating in 5-10 minute time resolution and occasionally down to 2-3 minutes, had been widely used to measure particle number size distributions (PNSDs) at the roadside. Dramatically varying PNCs at the roadside alone raise a challenge to measure PNSD accurately using such low time resolution scanning sizers, and the measured PNSD may be severely distorted from the real values (Yao et al., 2006a,b). In addition, PNSDs at the roadside can also vary because of the short distance between the sampling site and the traffic flow, e.g., the PNSDs sometimes represent an overwhelming contribution from the emissions of a single vehicle, but sometimes represent the combined contribution from a few vehicle emissions or the combined contribution from the traffic flow. Highly varying PNSDs at the roadside may further worsen the accuracy of the PNSDs measured by low time resolution scanning sizers. When a high time resolution particle sizer, e.g., Fast Mobility Particle Sizer (FMPS) or Engine Exhaust Particle Sizer (EEPS), is used, the uncertainty can be greatly reduced (Yao et al., 2006a,b). The measured PNSD in one-second time resolution can allow extraction of the new particle signal from the mixed signals of newly formed particles, pre-existing ambient particles and freshly emitted particles from combustion (Liu et al., 2014).

NPF has been recognized as a major contributor to the severe haze in Beijing (Guo et al., 2014). Furthermore, organic species have been shown to play a key role in the growth and aging of the nanoparticles (Peng et al., 2016). Ultrafine particles (<100 nm) have been implicated in adverse human health impacts through the deposition in the pulmonary region and penetration into the bloodstream (Oberdörster et al., 2004; Schlesinger et al., 2006; Zhang et al., 2012, 2015). On NPF days, the ultrafine particle number concentration is sharply increased, and potential health impacts are largely dependent on particle loadings (Guo et al., 2014). How enhancement and scavenging affect the net production of newly formed particles is still poorly understood, although numerous studies have focused mainly on the effects of enhancement and scavenging on nucleation rates or apparent formation rates observed for new particles. In addition, the newly formed particles inside a street

canyon might become toxic when organics released by vehicles are involved in the nucleation process (Sgro et al., 2009; Gualtieri et al., 2014).

In this study, we present simultaneous aerosol measurements at a street site and a rooftop site at a height of 20 m in winter and spring times in Beijing (Fig. 1). PNSDs at these two locations were measured by two identical FMPSs with one-second time resolution. We focused on analyzing the differences in apparent formation rates and particle yields of new particles between the street and rooftop sites to evaluate the effects of the street canyon on NPF. In addition, we also discuss the occurrence or absence of apparent growth in NPF events in terms of characteristics related to, for instance, warm or cold ambient temperatures and potential condensation vapors.

2. Method

2.1 Sampling sites, periods and meteorological conditions

Two urban sites, approximately 500 m from each other, were adopted for sampling in this study (Fig. 1). One site was 18 m from the curb of a heavily travelled (Chengfu) Road in the north-western area in Beijing. This site was physically located inside a street canyon, and is hereafter referred to as the street site. The daily average traffic volume on this road was 1.9×10^3 vehicles h^{-1} with a maximum of $2.2\text{-}2.4\times10^3$ vehicles h^{-1} in the morning and afternoon rush hours. A space-heating boiler with a stack ~50 m in height was approximately 200 m from the street site at the northeast. The site on the rooftop of an academic building inside the campus of Peking University (~20 m above ground level) was approximately 200 m from the nearest Zhongguancun North Street. The site is referred to as the rooftop site in this study and was assumed to represent the urban background.

Two sampling campaigns were conducted in winter 2011 and spring 2012, respectively. The winter sampling in 2011 included two phases, i.e., 1) only one FMPS operated during 10-15 December at the street site; and 2) two FMPSs operated during 16-23 December at the street site and rooftop site, respectively. The weather was typically sunny and dry during the sampling campaign with surrounding air temperatures from -9.5℃ to 12.8℃ (see Supplementary, Fig. S1). Relative humidity (RH) varied from 13% to 49% during the NPF days. During 12-17 April 2012, the two identical particle sizers were deployed at the rooftop site for intercomparison. The simultaneous measurements at two sites started from 18 to 27

April 2012. The ambient temperature ranged from 8.2℃ to 31.5℃ during the spring sampling period（Fig. S1). Sunny days occurred during 12-17 April and 25-27 April 2012 with ambient RH below 55%. Either rainy or cloudy days occurred for the remaining 7 days.

2.2 Sampling instruments

Two identical FMPSs (TSI, 3091) downstream of two dryers (TSI, 3062) were used in this study. FMPSs were used to continuously measure PNSDs with mobility diameters ranging from 5.6 nm to 560 nm at one-second time resolution, facilitating the investigation of rapid changes in nanoparticles due to formation and mixing from different sources (Yao et al., 2005, 2006b). Conductive tubes (TSI 3/8", each cut to a length of 2.8 m) were used for sampling at the two sites. The two FMPSs operated side-by-side during 12-17 April 2012 for intercomparison. The correlation coefficients (R^2) of the measured number concentrations between the two sizers were greater than 0.95 for particles with diameters of 9.3 nm-107.5 nm and 0.81 for particles in the size bin of 8.06 nm. However, the correlation coefficients are fairly small (< 0.3) for the remaining two size bins (6.04 nm and 6.98 nm) and are therefore discarded in the analysis. The relative error between the two FMPSs was less than 30% for 8.06 nm-107.5 nm particles (Table S1), and the difference for the measured number concentrations of particles with diameters larger than 8 nm was tested to be negligible by installing or removing the sampling line. However, the FMPS was reported to underestimate the particle sizes compared to the SMPS and HR-ToF-AMS (Lee et al., 2013). Zimmerman et al. (2015) proposed that an independent measurement of a Condensation Particle Counter (CPC) simultaneously with the FMPS can be used to correct the FMPS data accurately. In this study, a CPC (TSI, 3785) was operating simultaneously with an FMPS at the street site, and the FMPS was thereby used as the reference to correct the number concentration measured by the other. The correction is discussed in detail in the supplementary. The growth factors of < 50 nm particles were negligible under the RH levels on NPF days (Hämeri et al., 2000), and the effect of the dryers on the measured NPF events was not considered.

In addition to the two FMPS instruments and one CPC instrument measuring PNC, a few other instruments were deployed at the same time. For example, SO_2, NO_x, NO, O_3, CO_2, CO were measured and recorded every minute at the rooftop site close to the FMPS. Other available instruments, including aethalometer, DustTrak, Q-Trak photometer were

used for filter sampling or semi-continuously measurement of air pollutants at the street site. A meteorological station was located on the roof of one sixth-floor building approximately 50 m from the street site, measuring air temperature, RH, wind speed and direction. The solar radiation was measured by State Key Laboratory of Atmospheric Boundary Layer Physics and Atmospheric Chemistry (LAPC) (Hu et al., 2010, 2012).

2.3 Computational methods

In this study, particles less than 20 nm are defined as the nucleation mode (Kulmala et al., 2004). The apparent formation rate of new particles larger than 8 nm (FR, J_8), considering the coagulation and growth losses, is calculated based on Eq. (1) (Sihto et al., 2006):

$$J_8 = \frac{dN_{8-20}}{dt} + CoagS_{8-20} \cdot N_{8-560} + \frac{GR_{8-20}}{12} \cdot N_{8-20} + S_{losses} \quad (1)$$

where the coagulation loss for particles with mobility diameters of 8-20 nm ($CoagS_{8\text{-}20}$·$N_{8\text{-}560}$) is the sum of particle-particle inter- and hetero-coagulation rates calculated in the same manner as Yao et al. (2005). The growth loss is due to condensation growth ($GR_{8\text{-}20}$) out of the 8-20 nm size range during the calculation period. S_{losses} includes additional losses and is assumed to be zero in this study. Thus, J_8 reflects a combination result of nucleation and subsequent initial growth of new particles.

The apparent growth rate (GR) of new particles is determined by the slope of the fitted geometric median diameter of new particles (D_{pg}, calculated by Whitby et al., 1978; Zhu et al., 2014) during the growth duration shown in Eq. (2):

$$GR = \frac{\Delta D_{pg}}{\Delta t} \quad (2)$$

The condensation sink is the loss rate of condensable vapor molecules onto the pre-existing particles, which is calculated in a manner similar to the calculations of Dal Maso et al. (2005) and Kulmala et al. (2001, 2005):

$$CS = 2\pi D \int D_p \beta_M(D_p) n(D_p) dD_p = 2\pi D \sum_i \beta_M D_{pi} N_{pi} \quad (3)$$

where D is the diffusion coefficient, β_M is the transitional regime correction factor, D_{pi} is the particle diameter of size class i, and N_{p_i} is the particle number concentration in size class i.

Gas-phase sulfuric acid concentration was estimated based on global solar radiation (SR), SO_2 concentration and condensation sink (Petäjä et al., 2009):

$$[H_2SO_4] = k \cdot \frac{[SO_2] \cdot SR}{CS} \quad (4)$$

where k is a constant value of 2.3×10^{-9} m^2 W^{-1} s^{-1}. In this study, the mixing ratio of SO_2 was measured only on the rooftop as discussed in Section 2.2.

The contribution of sulfuric acid vapor to the particle growth from D_{p0} to D_{p1} can be expressed in Eq. (5), based on Kulmala et al. (2001):

$$R=([H_2SO_4]_{average}/C)\times 100\% \quad (5)$$

where $[H_2SO_4]_{average}$ is the mean concentration of H_2SO_4 during the entire growth period, and the concentration of condensable vapor (C) for particle growth from D_{p0} to D_{p1} is calculated following the procedure of Kulmala et al. (2001).

3. Results and Discussion

3.1 Overview of NPF events during two campaigns

The NPF events occurred frequently on the sampling days, 7 out of 16 days in spring 2012 and 7 out of 14 days in winter 2011 (Fig. 2), consistent with previous studies showing that spring and winter were the seasons with highest frequency of NPF events in Beijing (Wu et al., 2007; Wehner et al., 2008; Wang et al., 2017). In this study, regional NPF events represent NPF events lasting over 1 hour, and short-lived NPF events represent the NPF lasting only for 10-20 minutes.

During the spring campaign, the FRs at the rooftop site in regional NPF events ranged from 1.9 to 12.2 cm^{-3} s^{-1} on an average of 8.0±3.5 cm^{-3} s^{-1} (Table S2). Two different growth patterns of new particles were observed, i.e., Class I was characterized by a typical "banana shape" growth when the geometric median diameter of new particles (D_{pg}) was increased from about 10 nm to 30-60 nm in 3-10 hours, which occurred during 12-14 and 16 April with the GR of 6.4±3.1 nm h^{-1} (Figs.

2a and S2); Class II was characterized by the initial D_{pg} of new particles at about 11 nm and no apparent growth being observed during the next 6-8 hours until the signal of new particles dropped to negligible levels, which occurred on 15, 25 and 27 April (Fig. 2a). These two growth patterns have frequently been observed in Beijing (Wehner et al., 2004, 2008; Shi et al., 2007; Wu et al., 2007), with no evident difference for the FRs between Class I and Class II. At the street site, Class II NPF events were also observed on 25 and 27 April 2012, and the D_{pg} was maintained around 11 nm for 6-8 hours without apparent growth, consistent with the observed phenomenon on the rooftop (Fig. 3 a,b,e,f). The FRs in the regional NPF events were 1.9 cm^{-3} s^{-1} at both sites on 25 April, and 10.2 cm^{-3} s^{-1} on the rooftop versus 8.1 cm^{-3} s^{-1} at the street site on 27 April (Table S2). Four short-lived NPF events were observed only on 25 April 2012 and showed larger FRs (13-49 cm^{-3} s^{-1}) at the two sites. However, the FRs at the street site were decreased by 7%-50%. Class II NPF events had once been argued to be plume events in the literature. The number concentrations of Aitken mode relative to nucleation mode particles were negligible during the Class II NPF events, implying a negligible contribution from the plumes to the observed total number concentrations. Our detailed analysis in the supplementary information strongly indicates that Class II NPF events should be regarded as regional NPF events instead of plume events.

On the 7 NPF days in the wintertime, the FRs at the street site were 7.0±2.9 cm^{-3} s^{-1} (Table S2). The values were comparable to those in the springtime observed at the two sampling sites. All these observed NPF events in the wintertime were subject to Class II, i.e., the D_{pg} of new particles remained around 11 nm in the absence of apparent particle growth (Fig. 2b). Simultaneous NPF events were observed at two sites on 21, 22 and 23 December 2011 and the FRs were 0.9, 1.9 and 0.8 cm^{-3} s^{-1} on the rooftop, only 1/6-1/4 of those corresponding values at the street site, i.e., 4.0, 7.9 and 4.4 cm^{-3} s^{-1} (Table S2).

3.2 Reduced NPF at the street site in the springtime

On 25 and 27 April 2012, NPF events were simultaneously observed at the two sites and lasted for 6-8 hours (Fig. 3a,b,e,f). The long time for NPF implied that the events occurred on the regional or semi-regional scale. We first analyzed the stronger NPF on 27 April. The NPF event occurred at approximately 09:37-09:40 (local standard time is used in this paper) and was strongly associated with the increased speed of the northwest wind, i.e., from <1 m s^{-1} at 08:00 to >6 m s^{-1}

after 09:45 (Fig. S3). The mixing ratio of SO_2 was increased from 1.5 ppb to 3 ppb during the initial half hour of the event and then rapidly dropped down to <1 ppb for the remaining five hours (Fig. 3c). The nucleation mode PNC varied during the whole event with three peaks observed at ~10:20, ~11:30 and ~13:45, suggesting the heterogeneity of NPF, which was likely caused by the heterogeneity of precursors including sulfuric acid vapor, amine and/or other low volatile species on the regional scale (Zhang et al., 2012; Kulmala et al., 2013; Ehn et al., 2014). The FR of 8.1 cm^{-3} s^{-1} at the street site was slightly lower than the value of 10.2 cm^{-3} s^{-1} on the rooftop, the condensation sinks were 1.2±0.37 ($\times 10^{-2}$ s^{-1}) and 0.75±0.21 ($\times 10^{-2}$ s^{-1}) for the street site and rooftop site, respectively (Table S2), with the higher condensation sink at the street site partially responsible for the lower FR. Obvious differences were observed in the initial new particle burst time (defined as the time for the nucleation mode particles to reach the maximum number concentration) between these two sites, i.e., 25 minutes at the street site and 36 minutes at the rooftop site, leading to a larger increase in nucleation mode PNCs on the rooftop (Fig. 3c). This phenomenon was first observed in this study by adopting the high time resolution instrument. To estimate the net production of newly formed particles at the two sites, we defined t_0 as the time immediately before the apparent NPF was initially observed and t_1 as the time when the nucleation mode PNC reaches the maximum value. The net maximum increase in nucleation mode PNC (NMINP) was calculated as $N_{8\text{-}20nm}(t_1)$-$N_{8\text{-}20nm}(t_0)$. The NMINP at the street site was reduced by 30% relative to the NMINP on the rooftop (Fig. 3c,d), implying the reduced NPF at the street site.

On 25 April, NPF events were also associated with a high wind speed of the northwest wind (Fig. S4). Four short-lived NPF events together with one regional NPF event were observed at both sites (Fig. 3e-h). Each short-lived NPF event lasted for only 10-20 minutes (e.g., 10:07-10:26, 10:27-10:36, 10:38-11:02, 11:40-11:50 in Fig. 3f) concurrently with spikes of SO_2 at 1-2 ppb, but the calculated FRs were high, i.e., 14-49 cm^{-3} s^{-1} at the rooftop site and 13-38 cm^{-3} s^{-1} at the street site. The short-lived events strongly implied a key role for the sulfuric acid vapor in NPF and the heterogeneity of NPF in both horizontal and vertical directions.

The regional NPF event on 25 April lasted for ~8 hours with varying nucleation mode PNCs. On the rooftop, a longer new particle burst time and higher PNC were observed (Fig. 3g), similar to those parameters observed on 27 April 2012. The FRs of 1.9 cm^{-3} s^{-1} were similar between the two sites. The calculated condensation sinks were 0.65±0.23($\times 10^{-2}$ s^{-1}) and 0.16±0.02($\times 10^{-2}$ s^{-1}) at the street site and rooftop site, respectively. The larger condensation sink at the street site was

partially responsible for the reduced NPF during the four short-lived events, but did not affect the FR in the regional NPF event. However, the NMINP at the street site was reduced by 24%, due mainly to the shorter initial new particle burst time (Fig. 3h).

The simple comparison, referred to as Evidence 1 in the latter discussion, might be insufficient to confirm the reduced NPF at the street site because of the complicated micrometeorology such as different scale turbulences therein. Micrometeorology at street sites may cause accumulation or dilution of atmospheric particles. To solidify the reduced NPF at the street site, we provided two types of additional evidences that were less affected by the micrometeorology at the street site.

Evidence 2-3 were obtained by subtracting the PNC of different-sized particles at the rooftop site from the corresponding PNC at the street site, and the size-segregated difference in PNC between the two sites in April was thereby calculated (Fig. 4). The difference was largely negative for particles <14 nm during the NPF periods on 25 and 27 April (solid lines) against the positive difference of Aitken mode particles. In contrast, such a difference was slightly positive for particles <14 nm during the non-NPF days and during the morning rush hours on 25 and 27 April prior to the occurrence of NPF events (Fig. 4, dashed lines), because of increasing contributions from on-road vehicles at the street site as well as the accumulation effect associated with the micrometeorology at the street site. The same accumulation effect should theoretically exist during the NPF periods on 25 and 27 April, but the observed result showed the reverse. We thus obtained Evidence 2, i.e., the negative difference of nucleation mode particles on NPF days against the positive difference of nucleation mode particles on non-NPF days. Considering the positive difference of Aitken mode particles during the NPF periods on 25 and 27 April (solid lines), we can infer that micrometeorology favored an increase in nucleation mode particle number concentration at the street site. However, the observed result was contradictory to the interference. We thus obtained Evidence 3, i.e., the negative difference of nucleation mode particles on NPF days against the positive difference of those Aitken mode particles.

Overall, the reduced NPF events were always observed at the street site and supported by three types of Evidence 1-3. Although the number of the cases was not large, the reduced NPF events at the street site were theoretically expected on the basis of well-recognized factors in the literature, e.g., 1) a larger condensation sink associated with more pre-existing

atmospheric particles from primary emissions, 2) tall buildings along both sides of the urban streets can provide additional surface areas to scavenge gases and atmospheric particles (Yao et al., 2011), and 3) vehicle-emitted NO reacting with RO_2 and suppressing NPF (Wildt et al., 2014).

3.3 Enhanced NPF at the street site in the wintertime

On 21-23 December 2011, NPF events were simultaneously observed at the rooftop site and street site with the FRs of 0.8-1.9 cm^{-3} s^{-1} and 4.0-7.9 cm^{-3} s^{-1}, respectively (Figs. 5 and S5). The different FRs implied that NPF was always greatly enhanced at the street site, which was referred to as Evidence 1 for the enhanced NPF in the latter discussion. Larger condensation sinks were, however, calculated at the street site (1.3×10^{-2} s^{-1} at the street site and $0.45\text{-}0.98\times10^{-2}$ s^{-1} at the rooftop site, Table S2), implying the influence of the larger condensation sink on NPF apparently overwhelmed by unknown factors.

The strongest NPF event was observed on 22 December. The NPF event initially observed at 09:40-09:45 at both sites (Fig. 5a-d) was also apparently correlated with the increasing speed of the northwest wind (Fig. S6). The initial new particle burst time periods were different at the two sites. For example, nucleation mode PNCs at the rooftop site were gradually increased from 0.2×10^{4} cm^{-3} at that time to the maximum value of 1.4×10^{4} cm^{-3} during the initial 2 hours (Fig. 5c). At the street site, vehicle emissions frequently influenced the sampling site, leading to numerous spikes in PNC and large uncertainty in calculating the FR. We thus used the 25% minimum coefficient of variation (CV) in PNCs as an indicator to eliminate the vehicle spikes (see supplementary for the calculation method). The results showed that the nucleation mode PNC increased rapidly within the initial 26 minutes and then decreased. The FR of 7.9 cm^{-3} s^{-1} at the street site was three times larger than the FR of 1.9 cm^{-3} s^{-1} on the rooftop. The larger FR at the street site was associated mainly with a shorter time for the new particle burst. The NMINP at the street site during the whole NPF event was approximately 50% higher than the NMINP on the rooftop (Fig. 5d). When the nucleation mode PNC at the street site reached the maximum, the corresponding PNC on the rooftop was only one-third of its own maximum value. The different increasing patterns of nucleation mode particles at two sites strongly indicated that they were subject to different NPF mechanisms.

We also directly deducted the contribution of vehicle spikes using the second approach described in the supplementary. The newly obtained PNCs at the street site are shown in Fig. 6a. The results obtained from the new approach showed: 1) the initial new particle burst time was 30 minutes, 2) the calculated FR was 7.0 cm^{-3} s^{-1}, and 3) the NMINP was 61% higher than the NMINP on the rooftop. The results agreed reasonably with the previous results using the 25% minimum CV (Fig. 6b). The two approaches strongly implied NPF being greatly enhanced at street site.

Black carbon (BC) or NO_x were also proposed to deduct the contribution of vehicle spikes (Fruin et al., 2004; Wang et al., 2012). The measured concentration of BC was thereby tried for deduction and very poor correlation was obtained because one-minute time resolution cannot allow successfully capture of vehicle spikes varying over a few seconds (see supplementary). With such poor correlation, the regression equation between PNC and BC was invalid for accurate deduction of the contribution from vehicle spikes. Theoretically, the correlation could be improved substantially with increasing distance of the sampling site from traffic-heavy roads because of fewer dynamic changes in PNC and PNSD (Zhu et al., 2002a,b, 2006). Although the two approaches used in this study may still suffer from uncertainty to some extent, they should be much better than those reported in the literature.

On 21 December 2011, the NPF event at the street site was also characterized by a shorter initial new particle burst time and a larger FR (Fig. 5e-h). Using the 25% minimum CV approach, the NMINP at the street site was 24% higher than the NMINP on the rooftop (Fig. 5h). When the nucleation mode PNC at the street site reached the maximum, the corresponding PNC on the rooftop was only one-fifth of its own maximum value. The NMINP at the street site was 46% large than the NMINP at the rooftop site on 23 December (Fig. S5). The second approach was invalid in those two days because of the weak NPF events.

We seek further additional evidence to support the enhanced NPF at the street site while the evidence should be less affected by the complicated micrometeorology. We also calculated the difference in PNC between the two sites in December 2011 using the number concentrations at the street site subtracting the corresponding concentration at the rooftop site (Fig. 7). Theoretically, larger condensation sinks should cause stronger scavenging effects at the street site during the NPF periods in the wintertime than in the springtime. However, the difference in the nucleation mode particles in the wintertime was positive. We then obtained Evidence 2 to solidify the enhanced NPF at the street site, i.e., the positive difference of the

nucleation mode particles in the wintertime against the negative difference in the springtime on NPF days. In Fig. 7, on the strongest NPF day (22 December), the positive difference for <20 nm particles during the NPF periods was evidently larger than the difference obtained approximately two hours prior to the NPF. The reverse was true for 20-80 nm particles. The former larger difference was unlikely to be due to the low-ambient-temperature-favored stronger formation of primary vehicular particles during the initial 1-2 second dilution (Burgard et al., 2006; Bishop et al., 2010) and the poor dispersion conditions because of the higher ambient temperature and larger wind speed during the NPF period. The differences for <20 nm particles during the NPF period on 22 December were larger than the differences averaged over non-NPF days (17-19 December) in December and the average value observed on 20 December alone, when the most frequent spikes of vehicular particles occurred among all non-NPF days in December, at the corresponding particle size ranges. We thereby obtained Evidence 3, i.e., the larger positive difference in the nucleation mode particles on NPF days against those on non-NPF days in the wintertime (Fig. 7). All three findings indicated the NPF being enhanced at the street site on 22 December. When the vehicular particle spikes during the NPF on 22 December were eliminated using the 25% minimum CV approach, the newly obtained difference also supported the NPF being enhanced at the street site. The differences for <20 nm particles on 21 and 23 December during the NPF were also positive, but the NPF events on the two days were weak.

3.4 Analysis of NPF being enhanced at the street site

Varying FRs, sulfuric acid concentrations and condensation sinks during the two measurement campaigns are shown in Fig. 8. The calculated concentrations of sulfuric acid were between 2×10^6 and 2×10^7 cm^{-3} during NPF periods, which was comparable to previous observations in Beijing (Yue et al., 2010; Zheng et al., 2011; Wang et al., 2017). Although the estimated concentrations of sulfuric acid were the highest on the rooftop in December when the calculated condensation sinks were comparable to those in April, the corresponding FRs were the smallest. Nucleation of sulfuric acid is well known to be enhanced by organics dominantly determining FRs in the urban atmosphere (Zhang et al., 2004, 2009; Wang et al., 2010). The smallest FRs at the rooftop site in December can be due to the lack of sufficient low-volatility organics or amines, which were possibly associated with low biogenic emissions at the low ambient temperature. However, the number of

datasets in this study was too small to yield a reasonable equation to link the calculated concentrations of sulfuric acid with FRs.

Relative to the rooftop site, the largely increased FRs at the street site in December were unlikely to be due to the increased concentrations of sulfuric acid. Our arguments are presented as below: 1) using the measurements in April as a reference, the concentrations of sulfuric acid were probably lower at the street site than at the rooftop site on the basis of lower FRs and larger condensation sinks at the street site, so the scavenging effect should also occur in December and lower the concentrations of sulfuric acid at the street site, and 2) in December, the mixing ratios of SO_2 at 1-2 hours immediately before NPF were 3-5 ppb at the rooftop site. The SO_2 was mainly from domestic heating, and the traffic-derived SO_2 at the street site was roughly estimated to be <1.3 ppb according to the results in our previous studies (Meng et al., 2015a,b). The concentrations of sulfuric acid at the street site may very likely be close to or even lower than the concentration of sulfuric acid at the rooftop site since the stronger scavenging effect probably canceled out the traffic-derived contribution to sulfuric acid.

Combining possibly low emissions of biogenic precursors in December, stronger condensational sinks and larger FRs at the street site in December, we inferred that NPF enhancement at the street site in December was very likely due to the nucleation of H_2SO_4 enhanced by additional chemicals such as organics and amines from vehicle emissions. There is a need for further simultaneous measurements of vapor precursors such as HOMs and organic acids (Zhao et al., 2009) and chemical compositions of particles about 10 nm at the rooftop site and street site simultaneously.

3.5 Limiting factors for the growth of new particles

The two particle growth patterns of NPF events are discussed further. The new particles in Class I and Class II may exert severe health problems to human beings considering its large PNC. In the meantime, the new particles in Class I could potentially have impacts on climate through radiation feedback. Theoretically, the GR of new particles is largely dependent on the amount of condensable vapors conquering the thermodynamic force plus the Kelvin Effect. The amounts of condensable vapors are determined by the emission rates of vapor precursors, photochemical reactions of the precursors and scavenging rates through the gas-particle condensation and deposition.

In Class I (which was observed only in April), sulfuric acid condensation was estimated to account for only 2.3%-18% of the new particle growth, which was consistent with previous studies in Finland and Mexico (Smith, et al., 2008). All NPF events in December were subject to Class II when the estimated concentrations of sulfuric acid were larger than the estimated concentrations of sulfuric acid in April. It is reasonable to say, therefore, sulfuric acid was not the crucial species in determining the two particle growth patterns.

As reported in the literature, the oxidation products of biogenic organic gases likely overwhelmingly determined the condensation growth of newly formed particles between 10-50 nm (Riipinen et al., 2011; Pierce et al., 2012; Schobesberger et al., 2013; Ehn et al., 2014; Liu et al., 2014; Ortega et al., 2015; Tröstl et al., 2016). In this study, the north or northwest wind dominated during the NPF periods, and the north and northwest directions of the sampling site subject to mountain areas have a high percentage of land-covered forests. Extensive biogenic VOCs are theoretically expected in spring and may act as important precursors in NPF. No apparent growth of newly formed particles with diameters of about 11 nm in Class II in December was possibly relative to the low biogenic emissions of organic gases in cold seasons. The hypothesis was not applicable for Class II in April. NPF events in April occurred in sunny, windy and warm days, regardless of Class I and Class II. Moreover, there were no significant difference for condensation sinks between in Class I and Class II, suggesting that the scavenging effect may not be the key factor in determining the presence or absence of the apparent new particle growth. To further understand the mechanism modulating the differences between Class I and Class II, photochemical reactions are discussed as follows. As shown in Fig. 2, the mixing ratio of (NO_2+O_3) in Class I was generally larger than the mixing ratio of (NO_2+O_3) in Class II, indicating that Class II in April may be related to weaker photochemical reactions, albeit uncertainty exists (i.e., the mixing ratio of (NO_2+O_3) was 40-50 ppb on 12 April concomitant with particle growth, comparable to that in Class II).

When four NPF events in Class I were examined, the observed growth rates of new particles with diameters larger than 10 nm were very low (0-0.6 nm h^{-1}) in the initial 20-70 minutes and then increased rapidly to 2.2-9.3 nm h^{-1} in the next 2-7 hours (Fig. S2). The smooth variations of NO_2+O_3 cannot explain the sudden and rapid growth of new particles after the initial 20-70 minutes. Alternatively, the sudden shift of the gas-particle system equilibrium seemed to be the reason. When the product of gases started to be larger than the thermodynamic equilibrium constant plus the Kelvin Effect term, the

reaction should proceed to the solid state, i.e., the gases start to partition on the particle phase, leading to the sudden growth of new particles, also implying that semivolatile species may play a role in the particle growth.

As mentioned earlier, there was no evident difference for the FRs between Class I and Class II in April. We can infer that the organics driving the apparent growth of new particles with diameters larger than 10 nm were probably different from the organics involved in nucleation (Kulmala and Kerminen, 2008; Zhang, 2010). That also applies to the case without apparent growth of new particles with the increased FRs at the street site in December.

Again, it is difficult to detect the organic and inorganic species in 10-50 nm particles (Smith, et al., 2008; Yue et al., 2010; Bzdek et al., 2012). The same can be said to confirm the actual organics driving the growth of new particles with diameters larger than 10 nm. Oxidized anthropogenic VOCs could theoretically participate in the growth of newly formed particles while the study is limited (Zhang et al., 2009; Hoyle et al., 2011), but the role of oxidized anthropogenic VOCs needs further study.

3.6 Relationship between FR and new particle yield

Sulfuric acid vapor has been identified as a key component for nucleation in urban atmospheres (Weber et al., 1996; Kulmala, 2003; Berndt et al., 2005; Fiedler et al., 2005). Supposing that sulfuric acid vapors are completely nucleated, followed by the nucleated particles growing to the detectable size, the yields of newly formed particles are determined mainly by the supply of sulfuric acid vapor and are less affected by the formation rate. However, it will take a long time to completely convert sulfuric acid vapor to new particles at a slow formation rate. In the atmosphere, sulfuric acid vapor, newly formed clusters and particles can be largely scavenged by preexisting particles. The increased formation rate favors coagulation growth of new particles with diameters less than 8 nm, shortening the time of new particles growing to be over 8 nm (detectable in this study) and therefore increase the conversion efficiency of sulfuric acid vapor to particles with diameters larger than 8 nm. How the increased formation rates affect the production of particles with diameters larger than 8 nm was examined below:

1) The FR was increased by ~3 times at the street site relative to the rooftop site on 22 December 2011, resulting in an additional increase in nucleation mode PNC by 4.9×10^3 cm^{-3}, equal to 50% of the NMINP at the rooftop site, 2) The FRs at

the street site were increased by ~4-5 times relative to the rooftop site on 21 and 23 December 2011, leading to additional increase in new particles by 1.1×10^3 cm^{-3} (equal to 24% of the NMINP at the rooftop site) and 2.1×10^3 cm^{-3} (equal to 46% of the NMINP at the rooftop site), respectively. The largely increased FRs apparently yielded a small influence on the NMINP.

To further explore the relationship between FR and new particle yield, we summarized 139 cases of NPF events (only four short-lived events in this study being included, all the others were subject to regional NPF events) from our published and unpublished database measured in Beijing, Qingdao and marginal seas of China, etc. (Fig. 9a, Liu et al., 2014; Zhu et al., 2014; Man et al., 2015; Guo et al., 2016). Considered 1) formation rate of new particles, e.g., $J=k_{NucOrg}[H_2SO_4]^m[NucOrg]^n$ (Zhang et al., 2012) where k_{NucOrg} is a constant, NucOrg represents organics involved in nucleation, and m and n are two integers, 2) the subsequent particle growth, and 3) H_2SO_4 vapor to be necessary for nucleation in ambient air except at the sea beach, two scenarios were analyzed. Scenario 1: H_2SO_4 vapor is relatively sufficient against NucOrg and J_8 is thereby determined mainly by the availability of NucOrg vapor. A good correlation is theoretically expected for J_8 and NMINP. Scenario 2: NucOrg vapor is relatively sufficient against H_2SO_4 vapor, and J_8 is thereby determined mainly by the availability of H_2SO_4 vapor. J_8 could be high, but the total yield of new particles could be low because of a rapid consumption of H_2SO_4 vapor. A poor or no correlation is theoretically expected for J_8 and NMINP. For the cases summarized in Fig. 9a, the FRs and the NMINP had a moderately good correlation under FRs $\leq$8 cm^{-3} s^{-1}, with r=0.76 and $p<0.01$. For the FRs >8 cm^{-3} s^{-1}, the two variables had no correlation. When the FR was increased from 1 to 8 cm^{-3} s^{-1}, the nucleation mode PNC was increased from 0.4×10^4 to 3.3×10^4 cm^{-3} according to the regression equation. The statistical response of the NMINP to the increased FR was stronger than the results observed at the street site in December. This observation allows speculating that the NMINP in most of the atmospheric observations was possibly determined by the concentration of sulfuric acid vapor slightly more than additional organics. To support the hypothesis, we plotted NMINP against the mixing ratios of SO_2 measured during part of the events (Fig. 9b). The correlations were positive when the limited datasets were arbitrarily separated into two categories, i.e., r=0.81 and $p<0.01$ for Category 1, r=0.65 and p=0.16 for Category 2. This comparison, of course, needs the data for both vapors (e.g., HOMs) and chemical composition in the nucleation mode particles to confirm in future. For the FRs >8 cm^{-3} s^{-1}, the concentration of additional organic vapor

appeared to overwhelmingly determine the FRs, and the NMINP appeared to be determined mainly by the concentration of sulfuric acid vapor instead of additional organics.

4. Conclusions

The simultaneous aerosol measurements at a street site and a rooftop site were conducted using two FMPSs at one-second time resolution during two seasons in Beijing. At the street site, the reduced NPF events always occurred in the springtime while the enhanced NPF events always occurred in the wintertime. In the springtime, the reduced NPF was characterized by 1) the lower PNC of nucleation mode particles at the street site mainly because of a shorter initial burst time, 2) the negative difference of nucleation mode particles against the positive difference of Aitken mode particles on NPF days, 3) the negative difference of nucleation mode particles on NPF days against the positive difference on non-NPF days. We inferred that the reduced NPF at the street site was likely attributed to the scavenging effect where pollutants emitted from on-road vehicles were accumulated. In contrast, the enhanced NPF at the street site relative to the rooftop site in the wintertime was observed and supported by 1) the significantly larger PNC of nucleation mode particles (24%-50% increasing) at the street site and a larger FR (3-5 times higher) mainly because of a shorter initial burst time, 2) the positive difference of nucleation mode particles in the wintertime against the negative difference of nucleation mode particles in the springtime on NPF days, 3) the larger positive difference of nucleation mode particles on NPF days against that on non-NPF days in the wintertime. Through in-depth analysis, the vastly increased FRs were arguably due to the nucleation of H_2SO_4 enhanced by additional chemicals such as organics and amines from vehicle emissions, although further validation including direct measurements of amines and HOMs in the newly formed particles are still needed.

Two growth patterns of new particles were observed and occurred seasonally during our measurements, i.e., Class I showed a clear “banana shape” growth of new particles and occurred only in the springtime (4 days of 7 NPF days), while Class II showed no apparent growth of new particles with diameters of about 11 nm and occurred in the springtime (3 days of 7 NPF days) and always in the wintertime. Sulfuric acid can explain only 2.3%-18% of the new particle growth in Class I, and therefore is unlikely to be the crucial species determining the two particle growth patterns. Through a comprehensive analysis and combining widely recognized contributions of oxidized biogenic organics in growing particles in the literature,

we suggest that semivolatile species oxidized from biogenic organics in the presence of strong photochemical reactions play an important role in the growth of new particles with diameters larger than 10 nm.

Acknowledgments

We would like to thank the support from grant National Program on Key Basic Research Project (973 Program, 2014CB953703) and National Natural Science Foundation of China (NFSC, 41576118). We thank Prof. Tong Zhu for the use of his instrument and acknowledge valuable comments from Prof. Ming Fang.

References:

Arnold, F., Pirjola, L., Rönkkö, T., Reichl, U., Schlager, H., Lähde, T., Heikkilä, J., and Keskinen, J.: First online measurements of sulfuric acid gas in modern heavy-duty diesel engine exhaust: Implications for nanoparticle formation, Environ. Sci. Technol., 46, 11227-11234, doi: 10.1021/es302432s, 2012.

Berndt, T., Böge, O., Stratmann, F., Heintzenberg, J., and Kulmala, M.: Rapid formation of sulfuric acid particles at near-atmospheric conditions, Science, 307, 698-700, doi:10.1126/science.1104054, 2005.

Bishop, G. A., Peddle, A. M., Stedman, D. H., and Zhan, T.: On-road emission measurements of reactive nitrogen compounds from three California cities, Environ. Sci. Technol., 44, 3616-3620, doi: 10.1021/es903722p, 2010.

Buccolieri, R., Gromke, C., Di Sabatino, S., and Ruck, B.: Aerodynamic effects of trees on pollutant concentration in street canyons, Sci. Total Environ., 407, 5247-5256, doi:10.1016/j.scitotenv.2009.06.016, 2009.

Burgard, D. A., Bishop, G. A., and Stedman, D. H.: Remote sensing of ammonia and sulfur dioxide from on-road light duty vehicles, Environ. Sci. Technol., 40, 7018-7022, doi:10.1021/es061161r, 2006.

Bzdek, B. R., Zordan, C. A., Pennington, M. R., LutherIII, G. W., and Johnston, M. V.: Quantitative assessment of the sulfuric acid contribution to new particle growth, Environ. Sci. Technol., 46, 4365-4373, doi:10.1021/es204556c, 2012.

Dal Maso, M., Kulmala, M., Riipinen, I., Wagner, R., Hussein, T., Aalto, P. P., and Lehtinen, K. E. J.: Formation and growth of fresh atmospheric aerosols: eight years of aerosol size distribution data from SMEAR II, Hyytiala, Finland, Boreal Environ. Res., 10, 323-336, 2005.

Ehn, M., Thornton, J. A., Kleist, E., Sipilä, M., Junninen, H., Pullinen, I., Springer, M., Rubach, F., Tillmann, R., Lee, B., Lopez-Hilfiker, F., Andres, S., Acir, I-H., Rissanen, M., Jokinen, T., Schobesberger, S., Kangasluoma, J., Kontkanen, J., Nieminen, T., Kurtén, T., Nielsen, L. B., Jørgensen, S., Kjaergaard, H. G., Canagaratna, M., Dal Maso, M., Berndt, T., Petäjä, T., Wahner, A., Kerminen, V-M., Kulmala, M., Worsnop, D. R., Wildt, J., and Mentel, T. F.: A large source of low-volatility secondary organic aerosol, Nature, 506, 476-479, doi:10.1038/nature13032, 2014.

Fiedler, V., Dal Maso, M., Boy, M., Aufmhoff, H., Hoffmann, J., Schuck, T., Birmili, W., Hanke, M., Uecker, J., Arnold, F., and Kulmala, M.: The contribution of sulphuric acid to atmospheric particle formation and growth: a comparison between boundary layers in Northern and Central Europe, Atmos. Chem. Phys., 5, 1773-1785, doi:10.5194/acp-5-1773-

2005, 2005.

Fruin, S. A., Winer, A. M., and Rodes, C. E.: Black carbon concentrations in California vehicles and estimation of in-vehicle diesel exhaust particulate matter exposures, Atmos. Environ., 38, 4123-4133, doi:10.1016/j.atmosenv.2004.04.026, 2004.

Hämeri, K., Väkevä, M., Hansson, H. C., and Laaksonen, A.: Hygroscopic growth of ultrafine ammonium sulphate aerosol measured using an ultrafine tandem differential mobility analyser, J. Geophys. Res., 105(D17), 22231-22242, doi:10.1029/2000JD900220, 2000.

Gentner, D. R., Isaacman, G., Worton, D. R., Chan, A. W. H., Dallmann, T. R., Davis, L., Liu, S., Day, D. A., Russell, L. M., Wilson, K. R., Weber, R., Guha, A., Harley R. A., and Goldstein, A. H.: Elucidating secondary organic aerosol from diesel and gasoline vehicles through detailed characterization of organic carbon emissions, Proc. Natl. Acad. Sci, 109, 18318-18323, doi:10.1073/pnas.1212272109, 2012.

Gualtieri, M., Capasso, L., D'Anna, A., and Camatini, M.: Organic nanoparticles from different fuel blends: in vitro toxicity and inflammatory potential, J. Appl. Toxicol., 34, 1247-1255, doi:10.1002/jat.3067, 2014.

Guo, S., Hu, M., Zamora, M. L., Peng, J., Shang, D., Zheng, J., Du, Z., Wu, Z., Shao, M., Zeng, L., Molina, M. J., and Zhang, R.: Elucidating severe urban haze formation in China, Proc. Natl. Acad. Sci., 111, 17373-17378, doi:10.1073/pnas.1419604111, 2014.

Guo, T., Li, K., Zhu, Y., Gao, H., and Yao, X.: Concentration and size distribution of particulate oxalate in marine and coastal atmospheres-Implication for the increased importance of oxalate in nanometer atmospheric particles, Atmos. Environ., 142, 19-31, doi:10.1016/j.atmosenv.2016.07.026, 2016.

Hoyle, C. R., Boy, M., Donahue, N. M., Fry, J. L., Glasius, M., Guenther, A. Hallar, A. G., Huff Hartz, K., Petters, M. D., Petäjä, T., Rosenoern, T., and Sullivan, A. P.: A review of the anthropogenic influence on biogenic secondary organic aerosol, Atmos. Chem. Phys., 11, 321-343, doi:10.5194/acp-11-321-2011, 2011.

Hu, B., Wang, Y., and Liu, G.: Relationship between net radiation and broadband solar radiation in the tibetan plateau, Adv. Atmos. Sci., 29, 135-143, doi:10.1007/s00376-011-0221-6, 2012.

Hu, B., Wang, Y., and Liu, G.: Properties of ultraviolet radiation and the relationship between ultraviolet radiation and

aerosol optical depth in China, Atmos. Res., 98, 297-308, doi:10.1016/j.atmosres.2010.07.009, 2010.

Kittelson, D. B.: Engines and nanoparticles: a review, J. Aerosol Sci., 29, 575-588, doi:10.1016/S0021-8502(97)10037-4, 1998.

Kittelson, D. B., Watts, W. F., Johnson, J. P., Thorne, C., Higham, C., Payne, M., Goodier, S., Warrens, C., Preston, H., Zink, U., Pickles, D., Goersmann, C., Twigg, M. V., Walker, A. P., and Boddy, R.: Effect of fuel and lube oil sulfur on the performance of a diesel exhaust gas continuously regenerating trap, Environ. Sci. Technol., 42, 9276-9282, doi: 10.1021/es703270j, 2008.

Kulmala, M.: How particles nucleate and grow, Science, 302, 1000-1001, doi:10.1126/science.1090848, 2003.

Kulmala, M., Dal Maso, M., Mäkelä, J. M., Pirjola, L., Väkevä, M., Aalto, P., Miikkulainen, P., Hämeri, K., and O'Dowd, C. D.: On the formation, growth and composition of nucleation mode particles, Tellus B., 53, 479-490, doi:10.1034/j.1600-0889.2001.530411.x, 2001.

Kulmala, M., and Kerminen, V. M.: On the formation and growth of atmospheric nanoparticles, Atmos. Res., 90, 132-150, doi:10.1016/j.atmosres.2008.01.005, 2008.

Kulmala, M., Kontkanen, J., Junninen, H., Lehtipalo, K., Manninen, H. E., Nieminen, T., Petäjä, T.; Sipilä, M., Schobesberger, S., Rantala, P., Franchin. A., Jokinen, T., Järvinen, E., Äijälä, M., Kangasluoma, J., Hakala, J., Aalto, P. P., Paasonen, P., Mikkilä, J., Vanhanen, J., Aalto, J., Hakola, H., Makkonen, U., Ruuskanen, T., Mauldin III, R. L., Duplissy, J., Vehkamäki, H., Bäck, J., Kortelainen, A., Riipinen, I., Kurtén, T., Johnston, M. V., Smith, J. N., Ehn, M., Mentel, T. F., Lehtinen, K. E., Laaksonen, A., Kerminen, V. M., and Worsnop, D. R.: Direct observations of atmospheric aerosol nucleation, Science, 339, 943-946, doi:10.1126/science.1227385, 2013.

Kulmala, M., Petäjä, T., Mönkkönen, P., Koponen, I. K., Dal Maso, M., Aalto, P. P., Lehtinen, K. E. J., and Kerminen, V. M.: On the growth of nucleation mode particles: source rates of condensable vapor in polluted and clean environments, Atmos. Chem. Phys., 5, 409-416, doi:10.5194/acp-5-409-2005, 2005.

Kulmala, M., Vehkamäki, H., Petäjä, T., Dal Maso, M., Lauri, A., Kerminen, V. M., Birmili, W., and McMurry, P. H.: Formation and growth rates of ultrafine atmospheric particles: a review of observations, J. Aerosol Sci., 35, 143-176, doi:10.1016/j.jaerosci.2003.10.003, 2004.

Lee, B. P., Li, Y. J., Flagan, R. C., Lo, C., and Chan, C. K.: Sizing characterization of the fast mobility particle sizer (FMPS) against SMPS and HR-ToF-AMS, Aerosol Sci. Technol., 47, 1030-1037, doi:10.1080/02786826.2013.810809, 2013.

Liu, X. H., Zhu, Y. J., Zheng, M., Gao, H. W., and Yao, X. H.: Production and growth of new particles during two cruise campaigns in the marginal seas of China, Atmos. Chem. Phys., 14, 7941-7951, doi:10.5194/acp-14-7941-2014, 2014.

Liu, Y., Shao, M., Fu, L., Lu, S., Zeng, L., and Tang, D.: Source profiles of volatile organic compounds (VOCs) measured in China: Part I, Atmos. Environ., 42, 6247-6260, doi:10.1016/j.atmosenv.2008.01.070, 2008.

Man, H., Zhu, Y., Ji, F., Yao, X., Lau, N. T., Li, Y., Lee, B. P., and Chan, C. K.: Comparison of daytime and nighttime new particle growth at the HKUST supersite in Hong Kong, Environ. Sci. Technol., 49, 7170-7178, doi:10.1021/acs.est.5b02143, 2015.

Meng, H., Zhu, Y. J., Evans, G. J., and Yao X. H.: An approach to investigate new particle formation in the vertical direction on the basis of high time-resolution measurements at ground level and sea level, Atmos. Environ., 102, 366-375, doi:10.1016/j.atmosenv.2014.12.016, 2015a.

Meng, H., Zhu, Y. J., Evans, G. J., Jeong, C. H., and Yao, X. H.: Roles of SO_2 oxidation in new particle formation events, J. Environ. Sci., 30, 90-101, doi:10.1016/j.jes.2014.12.002, 2015b.

Merikanto, J., Spracklen, D. V., Mann, G. W., Pickering, S. J., and Carslaw, K. S.: Impact of nucleation on global CCN, Atmos. Chem. Phys., 9, 8601-8616, doi:10.5194/acp-9-8601-2009, 2009.

Oberdörster, G., Sharp, Z., Atudorei, V., Elder, A., Gelein, R., Kreyling, W., and Cox, C.: Translocation of inhaled ultrafine particles to the brain, Inhalation Toxicol., 16, 437-445, doi: 10.1080/08958370490439597, 2004.

Ortega, I. K., Donahue, N. M., Kurtén, T., Kulmala, M., Focsa, C., and Vehkamäki, H.: Can highly oxidized organics contribute to atmospheric new particle formation? J. Phys. Chem. A, 120, 1452-1458, doi:10.1021/acs.jpca.5b07427, 2015.

Peng, J., Hu, M., Guo, S., Du, Z., Zheng, J., Shang, D., Zamora, M. L., Zeng, L., Shao, M., Wu, Y., Zheng, J., Wang, Y., Glen, C. R., Collins, D. R., Molina, M. J., and Zhang, R.: Markedly enhanced absorption and direct radiative forcing of black carbon under polluted urban environments, Proc. Natl. Acad. Sci., 113, 4266-4271, doi: 10.1073/pnas.1602310113, 2016.

Petäjä, T., Mauldin III, R. L., Kosciuch, E., McGrath, J., Nieminen, T., Paasonen, P., Boy, M., Adamov, A., Kotiaho, T., and Kulmala, M.: Sulfuric acid and OH concentrations in a boreal forest site, Atmos. Chem. Phys., 9, 7435-7448, doi:10.5194/acp-9-7435-2009, 2009.

Pierce, J. R., Leaitch, W. R., Liggio, J., Westervelt, D. M., Wainwright, C. D., Abbatt, J. P. D., Ahlm, L., Al-Basheer, W., Cziczo, D. J., Hayden, K. L., Lee, A. K. Y., Li, S.-M., Russell, L. M., Sjostedt, S. J., Strawbridge, K. B., Travis, M., Vlasenko, A., Wentzell, J. J. B., Wiebe, H. A., Wong, J. P. S., and Macdonald, A. M.: Nucleation and condensational growth to CCN sizes during a sustained pristine biogenic SOA event in a forested mountain valley, Atmos. Chem. Phys., 12, 3147-3163, doi:10.5194/acp-12-3147-2012, 2012.

Pierson, W. R. and Brachaczek, W. W.: Emissions of ammonia and amines from vehicles on the road, Environ. Sci. Technol., 17, 757-760, doi:10.1021/es00118a013, 1983.

Qiu, C., and Zhang, R.: Multiphase chemistry of atmospheric amines, Phys. Chem. Chem. Phys. 15, 5738-5752, doi:10.1039/C3CP43446J, 2013.

Riccobono, F., Schobesberger, S., Scott, C. E., Dommen, J., Ortega, I. K., Rondo, L., Almeida, J., Amorim, A., Bianchi, F., Breitenlechner, M., David, A., Downard, A., Dunne, E. M., Duplissy, J., Ehrhart, S., Flagan, R. C., Franchin, A., Hansel, A., Junninen, H., Kajos, M., Keskinen, H., Kupc, A., Kürten, A., Kvashin, A. N., Laaksonen, A., Lehtipalo, K., Makhmutov, V., Mathot, S., Nieminen, T., Onnela, A., Petäjä, T., Praplan, A. P., Santos, F. D., Schallhart, S., Seinfeld, J. H., Sipilä, M., Spracklen, D. V., Stozhkov, Y., Stratmann, F., Tomé, A., Tsagkogeorgas, G., Vaattovaara, P., Viisanen, Y., Vrtala, A., Wagner, P, E., Weingartner, E., Wex, H., Wimmer, D., Carslaw, K, S., Curtius, J., Donahue, N. M., Kirkby, J., Kulmala, M., Worsnop, D. R., and Baltensperger, U.: Oxidation products of biogenic emissions contribute to nucleation of atmospheric particles, Science, 344, 717-721, doi:10.1126/science.1243527, 2014.

Riipinen, I., Pierce, J. R., Yli-Juuti, T., Nieminen, T., Häkkinen, S., Ehn, M., Junninen, H., Lehtipalo, K., Petäjä, T., Slowik, J., Chang, R., Shantz, N. C., Abbatt, J., Leaitch, W. R., Kerminen, V. M., Worsnop, D. R., Pandis, S. N., Donahue, N. M., and Kulmala, M.: Organic condensation: a vital link connecting aerosol formation to cloud condensation nuclei (CCN) concentrations, Atmos. Chem. Phys., 11, 3865-3878, doi:10.5194/acp-11-3865-2011, 2011.

Rönkkö, T., Lähde, T., Heikkilä, J., Pirjola, L., Bauschke, U., Arnold, F., Schlager, H., Rothe, D., Yli-Ojanpera, J., and

Keskinen, J.: Effects of gaseous sulphuric acid on diesel exhaust nanoparticle formation and characteristics, Environ. Sci. Technol., 47, 11882-11889, doi:10.1021/es402354y, 2013.

Schlesinger, R. B., Kunzli, N., Hidy, G. M., Gotschi, T., and Jerrett, M.: The health relevance of ambient particulate matter characteristics: coherence of toxicological and epidemiological inferences, Inhalation Toxicol., 18, 95-125, doi:10.1080/08958370500306016, 2006.

Schobesberger, S., Junninen, H., Bianchi, F., Lönn, G., Ehn, M., Lehtipalo, K., Dommen, J., Ehrhart, S., Ortega, I. K., Franchin, A., Nieminen, T., Riccobono, F., Hutterli, M., Duplissy, J., Almeida, J., Amorim, A., Breitenlechner, M., Downard, A. J., Dunne, E. M., Flagan, R. C., Kajos, M., Keskinen, H., Kirkby, J., Kupc, A., Kürten, A., Kurtén, T., Laaksonen, A., Mathot, S., Onnela, A., Praplan, A. P., Rondo, L., Santos, F. D., Schallhart, S., Schnitzhofer, R., Sipilä, M., Tomé, A., Tsagkogeorgas, G., Vehkamäki, H., Wimmer, D., Baltensperger, U., Carslaw, K. S., Curtius, J., Hansel, A., Petäjä, T., Kulmala, M., Donahue, N. M., and Worsnop, D. R.: Molecular understanding of atmospheric particle formation from sulfuric acid and large oxidized organic molecules, Proc. Natl. Acad. Sci., 110, 17223-17228, doi:10.1073/pnas.1306973110, 2013.

Sgro, L. A., Simonelli, A., Pascarella, L., Minutolo, P., Guarnieri, D., Sannolo, N., Netti, P, and D'Anna, A.: Toxicological properties of nanoparticles of organic compounds (NOC) from flames and vehicle exhausts, Environ. Sci. Technol., 43, 2608-2613, doi:10.1021/es8034768, 2009.

Shi, J. P., Mark, D., and Harrison, R. M.: Characterization of particles from a current technology heavy-duty diesel engine, Environ. Sci. Technol., 34, 748-755, doi:10.1021/es990530z, 2000.

Shi, Z. B., He, K. B., Yu, X. C., Yao, Z. L., Yang, F. M., Ma, Y. L., Ma, R., Jia, Y. T., and Zhang, J.: Diurnal variation of number concentration and size distribution of ultrafine particles in the urban atmosphere of Beijing in winter, J. Environ. Sci., 19, 933-938, doi:10.1016/S1001-0742(07)60154-5, 2007.

Sihto, S.-L., Kulmala, M., Kerminen, V.-M., Dal Maso, M., Petäjä, T., Riipinen, I., Korhonen, H., Arnold, F., Janson, R., Boy, M., Laaksonen, A., and Lehtinen, K. E. J.: Atmospheric sulphuric acid and aerosol formation: implications from atmospheric measurements for nucleation and early growth mechanisms, Atmos. Chem. Phys., 6, 4079-4091, doi:10.5194/acp-6-4079-2006, 2006.

Smith, J. N., Dunn, M. J., VanReken, T. M., Iida, K., Stolzenburg, M. R., McMurry, P. H., and Huey, L. G.: Chemical composition of atmospheric nanoparticles formed from nucleation in Tecamac, Mexico: Evidence for an important role for organic species in nanoparticle growth, Geophys. Res. Lett., 35, doi: 10.1029/2007GL032523, 2008.

Stemmler, K., Bugmann, S., Buchmann, B., Reimann, S., and Staehelin, J.: Large decrease of VOC emissions of Switzerland's car fleet during the past decade: results from a highway tunnel study, Atmos. Environ., 39, 1009-1018, doi:10.1016/j.atmosenv.2004.10.010, 2005.

Sun, Y. L., Zhang, Q., Schwab, J. J., Chen, W. N., Bae, M. S. Hung, H. M., Lin, Y. C., Ng, N. L., Jayne, J., Massoli, P., Williams, L. R., and Demerjian, K. L.: Characterization of near-highway submicron aerosols in New York City with a high-resolution aerosol mass spectrometer, Atmos. Chem. Phys., 12, 2215-2227, doi:10.5194/acp-12-2215-2012, 2012.

Tröstl, J., Chuang, W. K., Gordon, H., Heinritzi, M., Yan, C., Molteni, U., Ahlm, L., Frege, C., Bianchi, F., Wagner, R., Simon, M., Lehtipalo, K., Williamson, C., Craven, J. S., Duplissy, J., Adamov, A., Almeida, J., Bernhammer, A. K., Breitenlechner, M., Brilke, S., Dias, A., Ehrhart, S., Flagan, R. C., Franchin, A., Fuchs, C., Guida, R., Gysel, M., Hansel, A., Hoyle, C. R., Jokinen, T., Junninen, H., Kangasluoma, J., Keskinen, H., Kim, J., Krapf, M., Kürten, A., Laaksonen, A., Lawler, M., Leiminger, M., Mathot, S., Möhler, O., Nieminen, T., Onnela, A., Petäjä, T., Piel, F. M., Miettinen, P., Rissanen, M. P., Rondo, L., Sarnela, N., Schobesberger, S., Sengupta, K., Sipilä, M., Smith, J. N., Steiner, G., Tomè, A., Virtanen, A., Wagner, A. C., Weingartner, E., Wimmer, D., Winkler, P. M., Ye, P. L., Carslaw, K. S., Curtius, J., Dommen, J., Kirkby, J., Kulmala, M., Riipinen, I., Worsnop, D. R., Donahue, N. M., and Baltensperger, U.: The role of low-volatility organic compounds in initial particle growth in the atmosphere, Nature, 533, 527-531, doi:10.1038/nature18271, 2016.

Vu, T. V., Delgado-Saborit, J. M., and Harrison, R. M.: Review: Particle number size distributions from seven major sources and implications for source apportionment studies, Atmos. Environ., 122, 114-132, doi:10.1016/j.atmosenv.2015.09.027, 2015.

Wang, L., Khalizov, A. F., Zheng, J., Xu, W., Ma, Y., Lal, V., and Zhang, R.: Atmospheric nanoparticles formed from heterogeneous reactions of organics, Nature Geosci., 3, 238-242, doi:10.1038/ngeo778, 2010.

Wang, X., Westerdahl, D., Hu, J., Wu, Y., Yin, H., Pan, X., and Zhang, K. M.: On-road diesel vehicle emission factors for

nitrogen oxides and black carbon in two Chinese cities, Atmos. Environ., 46, 45-55, doi:10.1016/j.atmosenv.2011.10.033, 2012.

Wang, Z., Wu, Z., Yue, D., Shang, D., Guo, S., Sun, J., Ding, A., Wang, L., Jiang, J., Guo, H., Gao, J., Cheung, H. C., Morawska, L., Keywood, M., and Hu, M.: New particle formation in China: Current knowledge and further directions, Sci. Total Environ., 577, 258-266, doi:10.1016/j.scitotenv.2016.10.177, 2017.

Weber, R. J., Marti, J. J., McMurry, P. H., Eisele, F. L., Tanner, D. J., and Jefferson, A.: Measured atmospheric new particle formation rates: Implications for nucleation mechanisms, Chem. Eng. Commun., 151, 53-64, doi:10.1080/00986449608936541, 1996.

Wehner, B., Birmili, W., Ditas, F., Wu, Z., Hu, M., Liu, X., Mao, J., Sugimoto, N., and Wiedensohler, A.: Relationships between submicrometer particulate air pollution and air mass history in Beijing, China, 2004-2006, Atmos. Chem. Phys., 8, 6155-6168, doi:10.5194/acp-8-6155-2008, 2008.

Wehner, B., Wiedensohler, A., Tuch, T. M., Wu, Z. J., Hu, M., Slanina, J., and Kiang, C. S.: Variability of the aerosol number size distribution in Beijing, China: New particle formation, dust storms, and high continental background, Geophys. Res. Lett., 31, doi:10.1029/2004GL021596, 2004.

Whitby, K. T.: The physical characteristics of sulfur aerosols, Atmos. Environ., 12, 135-159, doi:10.1016/0004-6981(78)90196-8, 1978.

Wildt, J., Mentel, T. F., Kiendler-Scharr, A., Hoffmann, T., Andres, S., Ehn, M., Kleist, E., Müsgen, P., Rohrer, F., Rudich, Y., Springer, M., Tillmann, R., and Wahner, A.: Suppression of new particle formation from monoterpene oxidation by NO_x, Atmos. Chem. Phys., 14, 2789-2804, doi:10.5194/acp-14-2789-2014, 2014.

Wu, Z., Hu, M., Liu, S., Wehner, B., Bauer, S., Ma ßling, A., Wiedensohler, A., PetäJä, T., Dal Maso, M., and Kulmala, M.: New particle formation in Beijing, China: Statistical analysis of a 1-year data set, J. Geophys. Res., 112, doi: 10.1029/2006JD007406, 2007.

Yao, X., Chan, C. K., Lau, N. T., Lau, P. S., and Fang, M.: Possible sampling artifact in real time particle size distributions related to sampling rate, Aerosol Sci. Technol., 40, 1080-1089, doi:10.1080/02786820600979121, 2006a.

Yao, X. H., Choi, M. Y., Lau, N. T., Lau, A. P. S., Chan, C. K., and Fang, M.: Growth and shrinkage of new particles in the atmosphere in Hong Kong, Aerosol Sci. Technol., 44, 639-650, doi:10.1080/02786826.2010.482576, 2010.

Yao, X. H., Lau, N. T., Fang, M., and Chan, C. K.: On the time-averaging of ultrafine particle number size spectra in vehicular plumes, Atmos. Chem. Phys., 6, 4801-4807, doi:10.5194/acp-6-4801-2006, 2006b.

Yao, X. H., Lau, N. T., Fang, M., and Chan, C. K.: Real-time observation of the transformation of ultrafine atmospheric particle modes, Aerosol Sci. Technol., 39, 831-841, doi:10.1080/02786820500295248, 2005.

Yao, X. H., Lee, C. J., Evans, G. J., Chu, A., Godri, K. J., McGuire, M. L., Ng, A. C., and Whitelaw, C.: Evaluation of ambient SO_2 measurement methods at roadside sites, Atmos. Environ., 45, 2781-2788, doi:10.1016/j.atmosenv.2011.01.070, 2011.

Yue, D. L., Hu, M., Zhang, R. Y., Wang, Z. B., Zheng, J., Wu, Z. J., Wiedensohler, A., He, L. Y., Huang, X. F., and Zhu, T.: The roles of sulfuric acid in new particle formation and growth in the mega-city of Beijing, Atmos. Chem. Phys., 10, 4953-4960, doi:10.5194/acp-10-4953-2010, 2010.

Zhang, R.: Getting to the critical nucleus of aerosol formation, Science, 328, 1366-1367, doi:10.1126/science.1189732, 2010.

Zhang, R., Khalizov, A., Wang, L., Hu, M., and Xu, W.: Nucleation and growth of nanoparticles in the atmosphere, Chem. Rev., 112, 1957-2011, doi:10.1021/cr2001756, 2012.

Zhang, R., Suh, I., Zhao, J., Zhang, D., Fortner, E. C., Tie, X., Molina, L. T., and Molina, M. J.: Atmospheric new particle formation enhanced by organic acids, Science, 304, 1487-1490, doi:10.1126/science.1095139, 2004.

Zhang, R., Wang, G., Guo, S., Zamora, M. L., Ying, Q., Lin, Y., Wang, W., Hu, M., and Wang, Y.: Formation of urban fine particulate matter, Chem. Rev., 115, 3803-3855, doi:10.1021/acs.chemrev.5b00067, 2015.

Zhang, R., Wang, L., Khalizov, A. F., Zhao, J., Zheng, J., McGraw, R. L., and Molina, L. T.: Formation of nanoparticles of blue haze enhanced by anthropogenic pollution, Proc. Natl. Acad. Sci, 106, 17650-17654, doi:10.1073/pnas.0910125106, 2009.

Zhao, J., Khalizov, A., Zhang, R., and McGraw, R.: Hydrogen bonding interaction of molecular complexes and clusters of aerosol nucleation precursors, J. Phys. Chem. A, 113, 680-689, doi:10.1021/jp806693r, 2009.

Zheng, J., Hu, M., Zhang, R., Yue, D., Wang, Z., Guo, S., Li, X., Bohn, B., Shao, M., He, L., Huang, X., Wiedensohler, A.,

and Zhu, T.: Measurements of gaseous H_2SO_4 by AP-ID-CIMS during CAREBeijing 2008 campaign, Atmos. Chem. Phys., 11, 7755-7765, doi:10.5194/acp-11-7755-2011, 2011.

Zhu, Y., Hinds, W. C., Kim, S., and Sioutas, C.: Concentration and size distribution of ultrafine particles near a major highway, J. Air Waste Manag. Assoc., 52, 1032-1042, doi:10.1080/10473289.2002.10470842, 2002a.

Zhu, Y., Hinds, W. C., Kim, S., Shen, S., and Sioutas, C.: Study of ultrafine particles near a major highway with heavy-duty diesel traffic, Atmos. Environ., 36, 4323-4335, doi:10.1016/S1352-2310(02)00354-0, 2002b.

Zhu, Y., Kuhn, T., Mayo, P., and Hinds, W. C.: Comparison of daytime and nighttime concentration profiles and size distributions of ultrafine particles near a major highway, Environ. Sci. Technol., 40, 2531-2536, doi:10.1021/es0516514, 2006.

Zhu, Y. J., Sabaliauskas, K., Liu, X. H., Meng, H., Gao, H. W., Jeong, C-H., Evans, G. J., and Yao, X. H.: Comparative analysis of new particle formation events in less and severely polluted urban atmosphere, Atmos. Environ., 98, 655-664, doi:10.1016/j.atmosenv.2014.09.043, 2014.

Zimmerman, N., Jeong, C. H., Wang, J. M., Ramos, M., Wallace, J. S., and Evans, G. J.: A source-independent empirical correction procedure for the fast mobility and engine exhaust particle sizers, Atmos. Environ., 100, 178-184, doi:10.1016/j.atmosenv.2014.10.054, 2015.

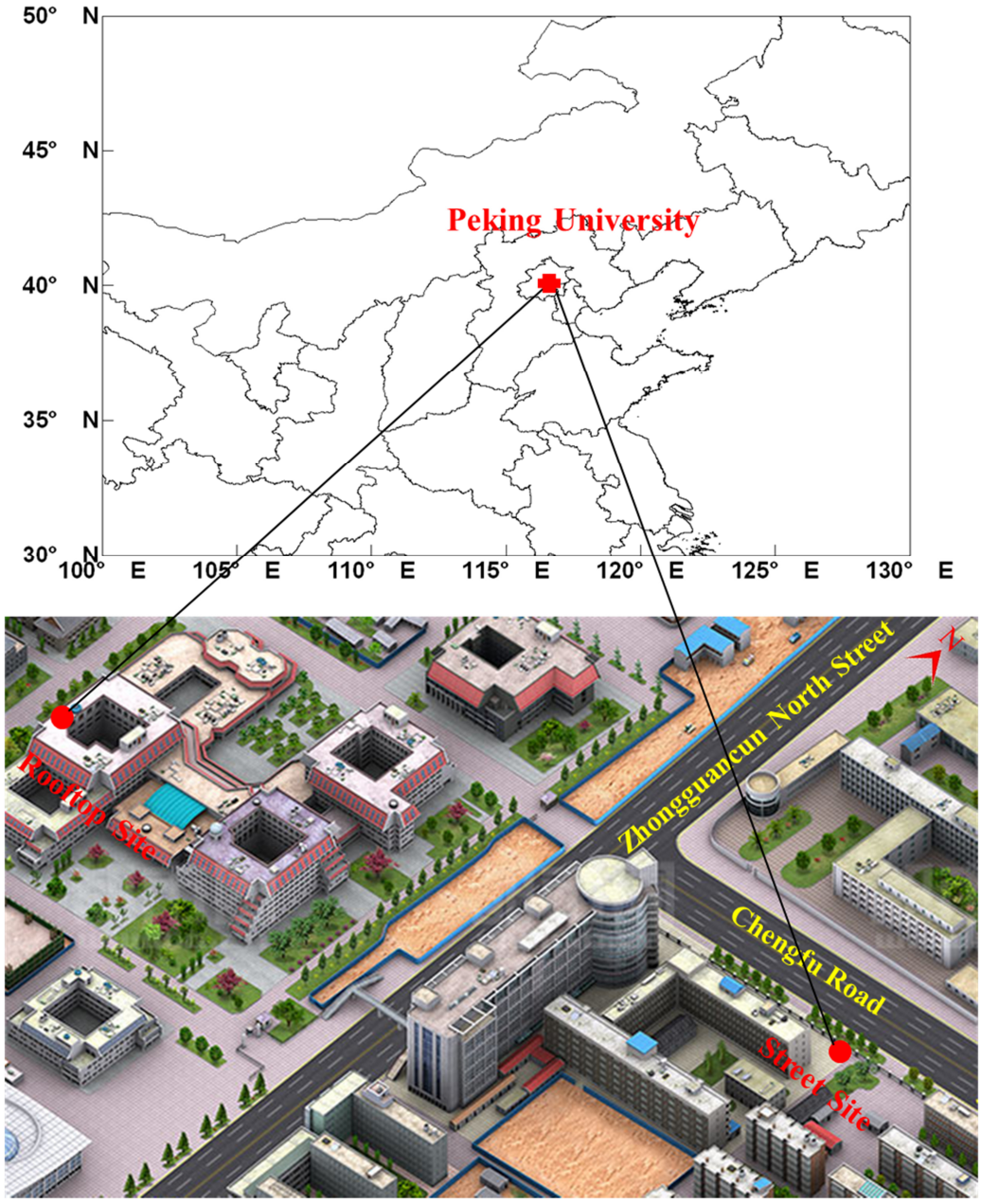

700

Fig. 1 The location of sampling sites (top) and 3D view of the two sampling sites (bottom, download from http://bj.o.cn/).

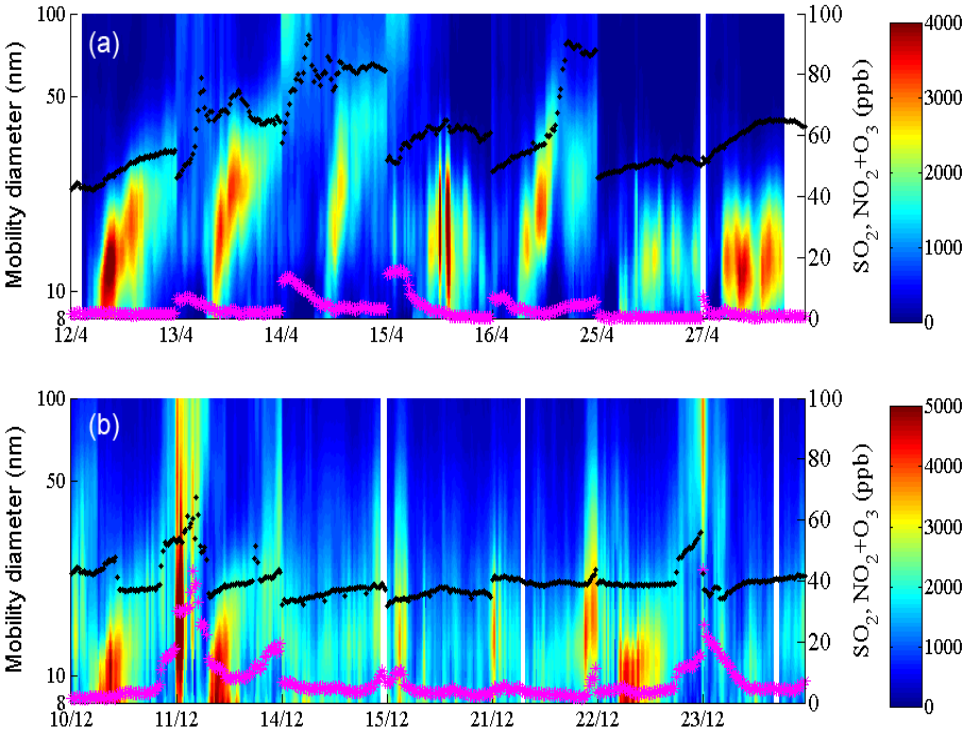

Fig. 2 Contour plots of particle number concentration (# cm^{-3}) and time series of NO_2+O_3 and SO_2 in the mixing ratio in two seasons (a: seven NPF events during 12-27 April 2012, b: seven NPF events during 10-23 December 2011; there were only data from 8:00 to 18:00 in each day to be shown, full black diamonds and peak magenta stars represent the mixing ratios of NO_2+O_3 and SO_2, repectively, while the values correspond to the right Y Axis).

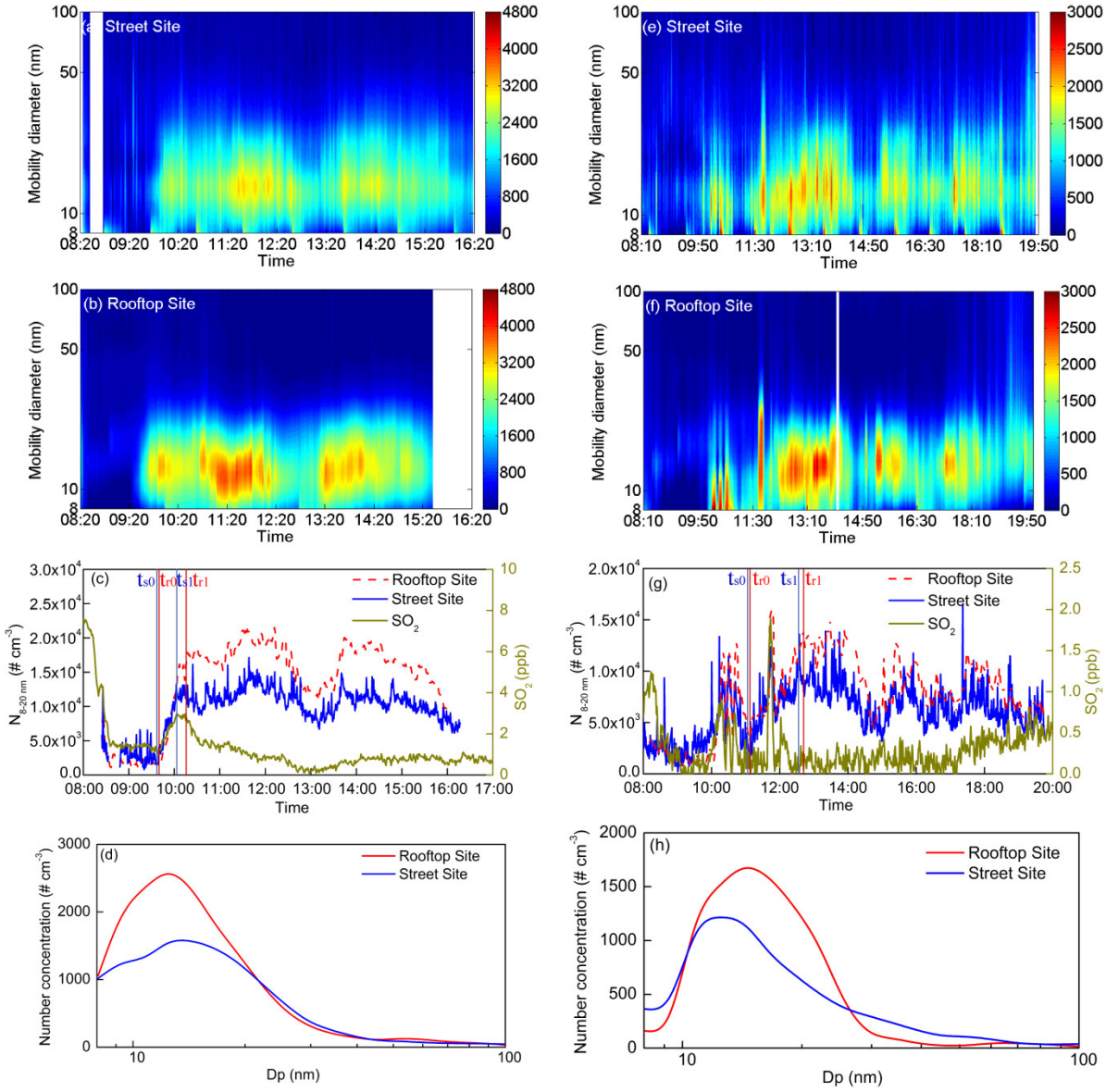

Fig. 3 Contour plots, time series of number concentrations and size distributions of atmospheric particles at two sampling sites on 27 April 2012 (left column) and 25 April 2012 (right column) (a, b, e, f: Contour plots of particle number concentration (# cm^{-3}); c, g: time series of nucleation mode PNC ($N_{8\text{-}20nm}$) and SO_2 mixing ratios at two sampling sites; d, h: size distributions of $N_{(ts1)}$-$N_{(ts0)}$ at the street site and $N_{(tr1)}$-$N_{(tr0)}$ on the rooftop, $N_{(ts1)}$-$N_{(ts0)\ and}$ $N_{(tr1)}$-$N_{(tr0)}$ represent the number concentration at each size bin at t_1 minus that at t_0 at the street site and at the rooftop site, respectively).

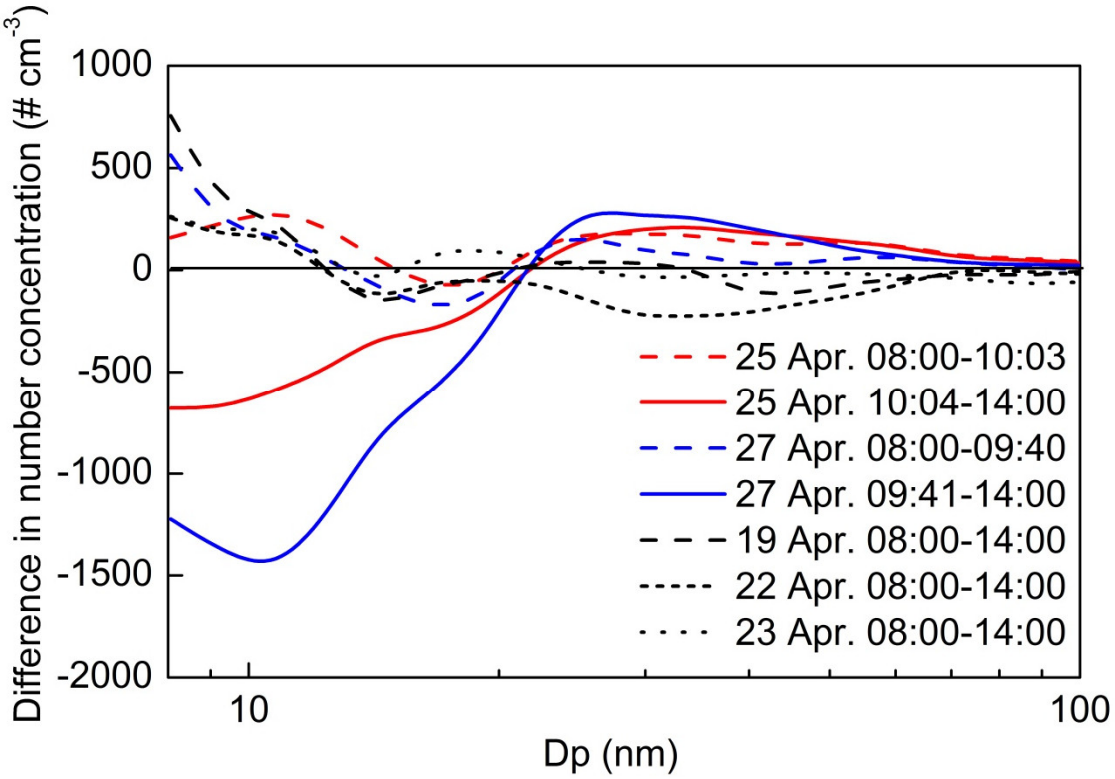

715 **Fig. 4** The size-dependent difference in number concentrations (calculated by the PNC of different sized particles at the street site subtracting the corresponding value at the rooftop site) during various periods in April 2012 (solid and dash lines represent the results during NPF and non-NPF periods, respectively).

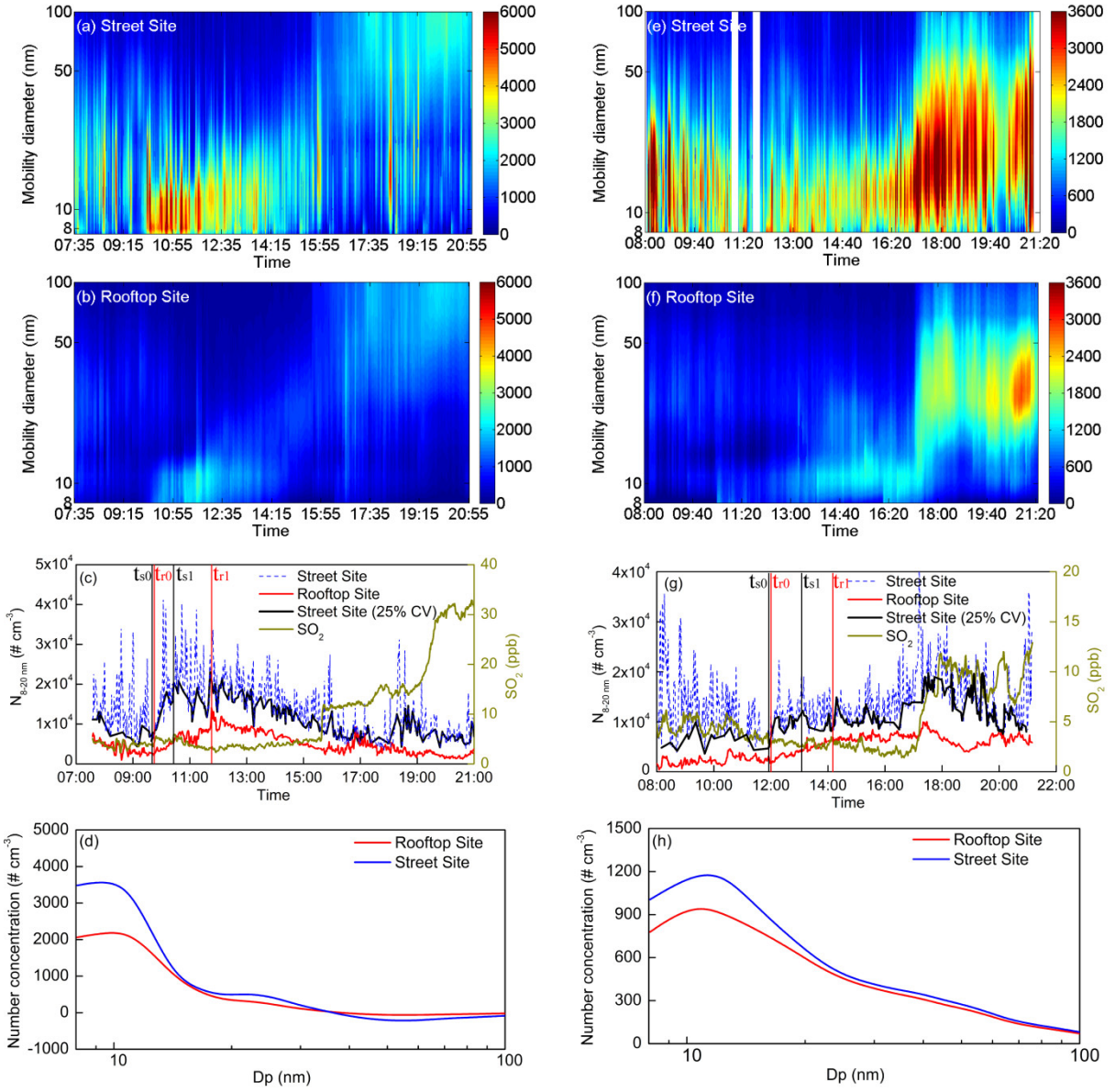

Fig. 5 Contour plots, time series of number concentrations and size distributions of atmospheric particles at two sampling sites on 22 December 2011 (left column) and 21 December 2011 (right column) (a, b, e, f: Contour plots of particle number concentration (# cm^{-3}); c, g: time series of nucleation mode PNC ($N_{8\text{-}20nm}$) and SO_2 mixing ratios at two sampling sites; d, h: size distributions of $N_{(ts1)}$-$N_{(ts0)}$ at the street site and $N_{(tr1)}$-$N_{(tr0)}$ on the rooftop).

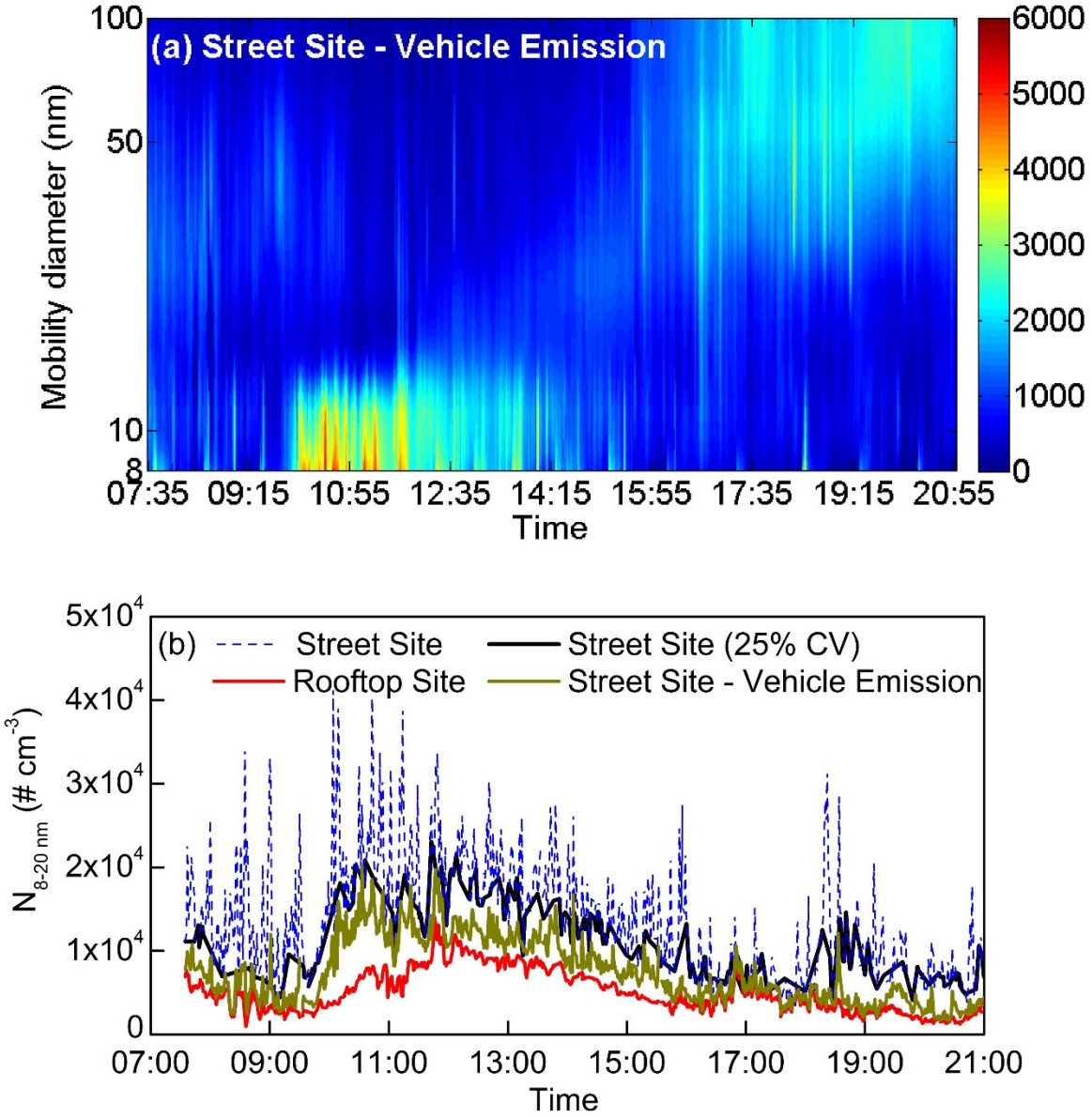

725 **Fig. 6** Contour plot and time series of particle number concentration with two approaches used to deduct freshly emitted traffic particles on 22 December 2011 (a: Contour plot of particle number concentration calculated from the second approach described in the supplementary; b: time series of number concentration at the street and rooftop site and those calculated from the two approaches defined in the context).

730

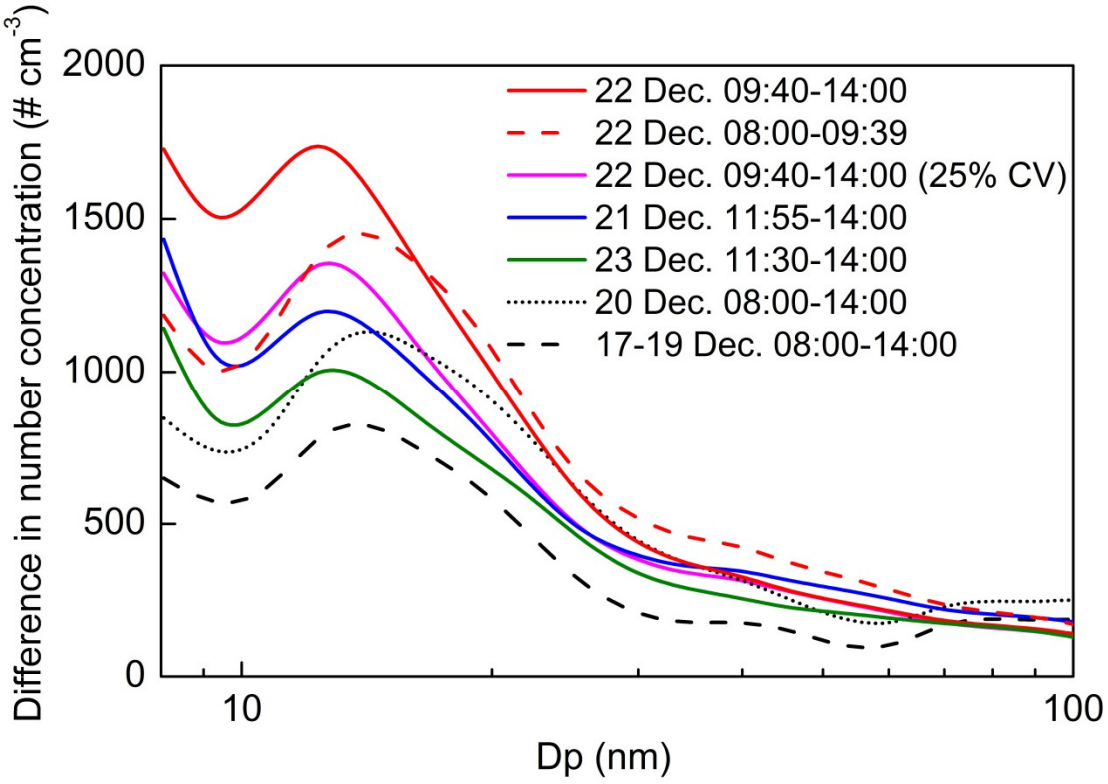

Fig. 7 The size-dependent difference in particle number concentrations between the two sites in December, 2011 (solid and dash lines represent the results during NPF and non-NPF periods, respectively).

735

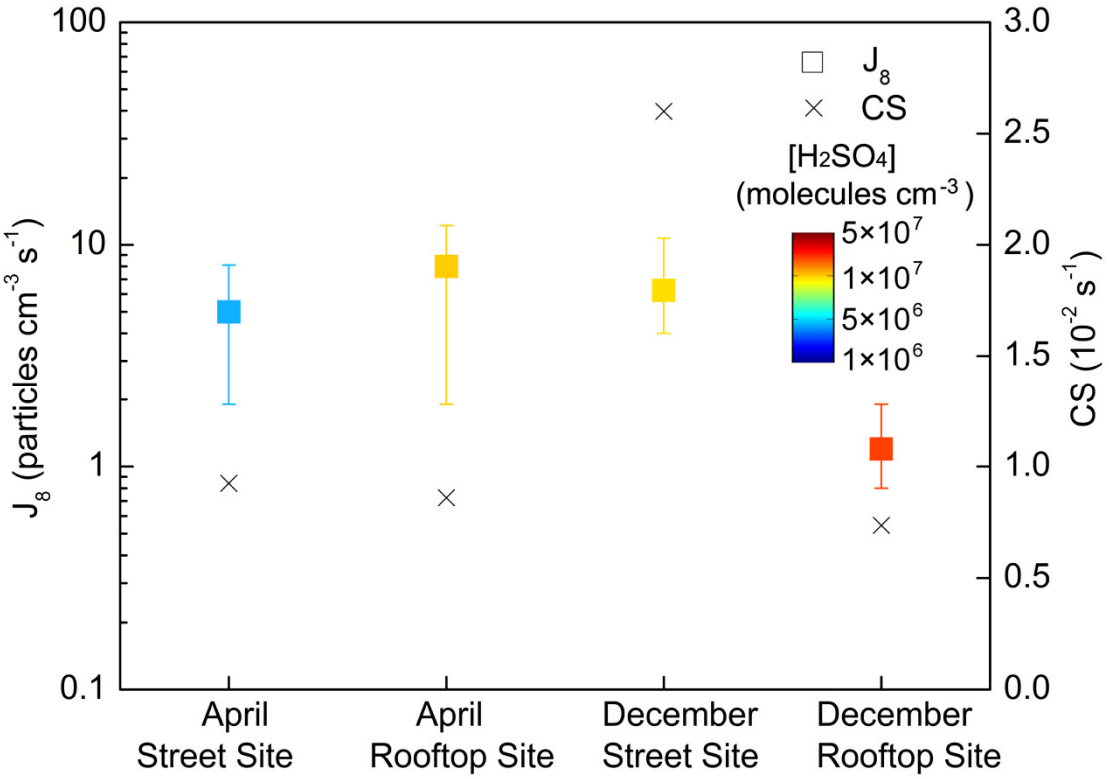

Fig. 8 Mean and range of FR (box symbol), condensation sinks (cross symbol) and estimated sulfuric acid concentrations (mean and standard deviation) in color bar on NPF days at two sites in April 2012 and December 2011 (The sulfuric acid at the street site was calculated by assuming the mixing ratio of SO_2 therein to be the same as that on the rooftop and the uncertainty on the estimation was analyzed in Supplementary).

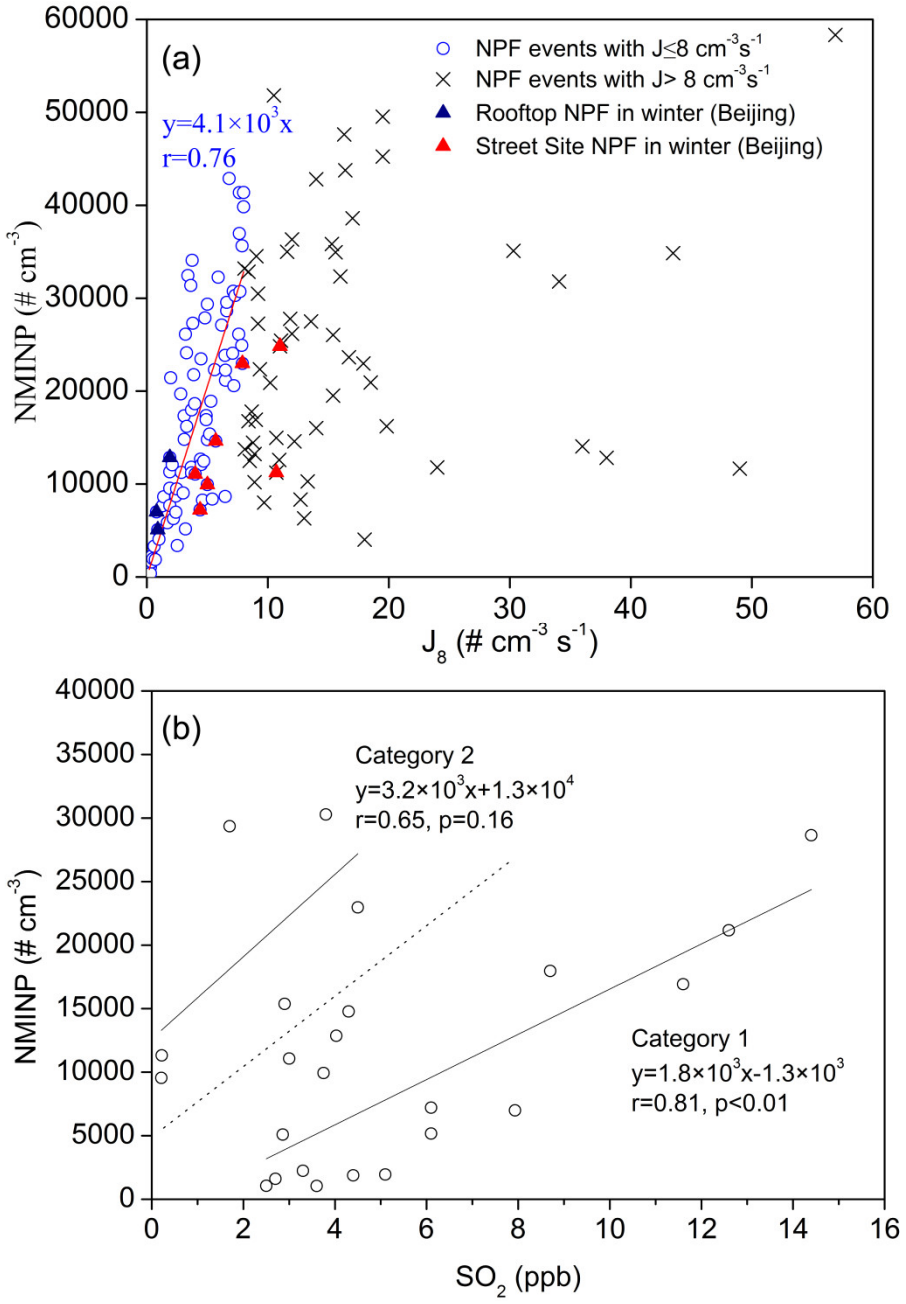

Fig. 9 Relationship between NMINP and FR (J_8) in 139 cases of NPF events and between NMINP and SO_2 in some cases (a: NMINP vs. FR (J_8); b: NMINP vs. SO_2; the dash line in Fig. b is arbitrarily drawn; the averaged mixing ratio of SO_2 during each NPF event was used, and missing SO_2 data are either due to malfunction of instruments or further QA/QC is required).